Physico-chemical characterization of urban aerosols from specific combustion sources in West Africa at Abidjan in Côte d'Ivoire and Cotonou in Benin in the frame of the DACCIWA program

Aka Jacques Adon[1], Catherine Liousse[1], Elhadji Thierno Doumbia[2], Armelle Baeza-Squiban[3], Hélène Cachier[1], Jean-Francois Léon[1], Veronique Yoboué[4], Aristique Barthel Akpo[5], Corinne Galy-Lacaux[1], Benjamin Guinot[1], Cyril Zouiten[6], Hongmei Xu[1, 7], Eric Gardrat[1], Sekou. Keita[8].

[1] Laboratoire d'Aérologie, Université de Toulouse, CNRS, UPS, Toulouse, France

[2] Centre National de Recherche Météorologique (CNRM)/Groupe d'étude de l'Atmosphère Météorologique, CNRS-Météo-France, Toulouse, France

[3] Université Paris Diderot, Unité de Biologie Fonctionnelle et Adaptative-RMCX, CNRS, UMR 8251, Paris, France

[4] Laboratoire de Physique de l'Atmosphère, Université Félix Houphouët-Boigny, Abidjan BPV 34, Côte d'Ivoire

[5] Laboratoire de Physique du Rayonnement, Université d'Abomey-Calavi, Abomey-Calavi, Bénin

[6] Géosciences Environnement Toulouse, Université de Toulouse, CNRS, UPS, Toulouse, France

[7] Department of Environmental Science and Engineering, Xi'an Jiaotong University, Xi'an, China

[8] Université de Khorogo, Khorogo, Côte d'Ivoire.

Correspondence to: adonjacks@gmail.com (J. Adon) and lioc@aero.obs-mip.fr (C. Liousse)

Abstract

Air pollution in West Africa has yet to be well characterized and was one of the principal motivations of the "Air Pollution and Health" work package in the DACCIWA (Dynamics-Aerosol-Chemistry-Cloud Interactions in West Africa) program. Intensive measurement campaigns were performed in two West African capitals (Abidjan in Côte d'Ivoire and Cotonou in Benin), in dry season (January 2016 and 2017) and wet season (July 2015 and 2016), in order to examine the size distribution of particulate matter (PM) and their chemical composition including elemental carbon (EC), organic carbon (OC), water-soluble organic carbon (WSOC), water-soluble inorganic ions (WSI) and trace metals. In this study, we characterize PM from different sites in Abidjan, which are representative of domestic fires (ADF), traffic (AT) and waste burning (AWB) sources and from one traffic site in Cotonou (CT). All these sites, impacted by large amount of pollution, are representative of the main combustion sources in South West Africa (SWA).

Results show very high PM concentrations at the SWA sites and a well-marked seasonality as well as a strong spatial variation. The average $PM_{2.5}$ mass concentrations during the wet season are 517.3, 104.1, 90.3 and 69.1 $\mu g.m^{-3}$ at the ADF, CT, AT and AWB sites, respectively. In the dry season, $PM_{2.5}$ concentrations decrease to 375.7 $\mu g.m^{-3}$ at the ADF site, while they increase to 269.7, 141.3 and 175.3 $\mu g.m^{-3}$ at the CT, AT and AWB sites, respectively. The annual $PM_{2.5}$ levels at almost all sites are significantly higher than the WHO guideline level of 10 $\mu g.m^{-3}$. As for PM mass, carbonaceous aerosol concentrations are also maximum at ADF site, accounting up to 69% of the total PM mass. The largest amount of these species on the ADF site in both seasons are due to the intensive human activities such as domestic cooking using wood and food smoking and roasting activities, known to be an important source of PM in SWA. Dust contributions are dominant at CT (57-80%), AT (20-70%) and AWB (30-69%) sites and specially in the coarse and fine particle modes at CT and in the coarse fraction at AT site, while there is no clear distribution at AWB site. This result reflects the specificity of most of SWA cities permanently impacted by dust emissions from the desert around and re-suspended particles from the roads. The contributions of WSI to the total PM mass are highly variable but remain less than 30%. Values are generally 1-3 times higher in the wet season than the dry season. The total proportion of WSI is driven by the individual contribution of three species such as chloride, nitrate and calcium, which may peak in the fine and/or large particles according to the site. This means that different types of sources (anthropogenic emissions from fuel combustion, nitrate formation by reaction processes and natural emissions) contribute to WSI emissions in the studied sites. The concentrations of element traces well reflect the trends

64   of dust at the traffic and AWB sites, with a predominance of Al, Na, Ca, Fe and K, keys markers
65   of crustal dust.

66   Our study highlights the contribution of different traffic emissions in two major West African
67   cities to atmospheric aerosol composition. It also highlights the role of domestic fires and waste
68   combustion sources. It constitutes an original database that characterizes urban air pollution
69   from specific African combustion sources.

70

71   **Keywords**: atmospheric pollution, chemical composition, physicochemical characterization,
72   Particulate matter, traffic, waste burning, domestic, biomass burning.

73

1.   Introduction

75   The impact of anthropogenic pollution on environment and health has been demonstrated by
76   numerous studies in Europe and North America, which have contributed to the implementation
77   of emission reduction policies. By contrast, air pollution in Africa is far from being well
78   characterized, although it is suspected to be responsible for negative health outcomes (*WHO,*
79   *2014*). This is a major problem since Africa is an intense emitter of pollution from
80   anthropogenic sources that includes domestic fires, vehicular traffic, waste burning as well as
81   growing oil and mining industries. It has also one of the fastest growing urban populations in
82   the world, especially in West and East Africa. As a consequence, it has been shown that massive
83   urbanization and rapid economic growth could be responsible for tripling anthropogenic
84   emissions in Africa between 2000 and 2030 (*Liousse et al., 2014*). Moreover, it is important to
85   recall the impact of biomass burning and dust sources in the African atmospheric composition,
86   especially occurring during the dry season. All of this results in a major degradation of urban
87   air quality and an impact on the health of exposed populations. Only a few studies on this
88   subject have been conducted in West Africa (*Val et al., 2013*; *Dieme et al., 2012*; *Kouassi et*
89   *al., 2009*) despite the high atmospheric pollutant concentrations already measured to be of the
90   same order as in Asian megacities and well above WHO international standards (*WHO, 2014*).

91   West Africa is then an "unique laboratory" to study urban pollution. Previous studies conducted
92   under the framework of the AMMA (Analyses Multidisciplinaires de la Mousson Africaine)
93   and POLCA (POLlution des Capitales Africaines) programs, have revealed very high
94   particulate pollution concentration levels in Cotonou (Benin), Bamako (Mali), Dakar (Senegal)

95   and Yaoundé (Cameroun) during the dry season (*Doumbia et al., 2012; Val et al., 2013*),
96   suggesting that the population may be affected by negative health outcomes. For example, *Val*
97   *et al. (2013)* showed that the inflammatory impact of combustion aerosol depends on the type
98   of emission sources and determined the predominant role of particulate organic matter.
99   Moreover, fine and ultrafine aerosol fractions, as well as their content in trace metals and
100 organic compounds, have been shown to induce biological effects due to their ability to reach
101 the distal lung (*Cassee et al., 2013*). Such reasons highlight the need to better understand the
102 size-speciation of aerosol chemical composition for the main West African anthropogenic
103 sources during the different seasons. Within this context, the DACCIWA (Dynamics-Aerosol-
104 Chemistry-Cloud Interactions in West Africa) program, dedicated a specific work package to
105 "Air Pollution and Health" dealing with pollutant characterization related to health issues
106 through toxicological studies and epidemiological studies.

107 Intensive and extensive campaigns have been organized from December 2014 to March 2017
108 in Abidjan and Cotonou. The strategy was to measure aerosol chemical composition in different
109 sites, representative of the main prevailing urban sources in West Africa following *Liousse et*
110 *al. (2014)* and *Keita et al. (2018)*. Two typical traffic-sampling sites were chosen, one in
111 Abidjan (Côte d'Ivoire) and another one in Cotonou (Benin), to take into account differences
112 in terms of fleets, type of fuel used and quality of roads. Indeed, in Cotonou, the majority of
113 population uses two-wheel vehicles susing gasoline fuel or gasoline and oil fuel, whereas in
114 Abidjan, the vehicle fleet is dominated by four-wheel engines using diesel fuel. Measurements
115 were also performed at domestic fire and waste burning sites, both located in Abidjan.

116 During the extensive campaign, PM$_{2.5}$ mass and carbonaceous aerosol were weekly measured
117 and results are discussed in *Djossou et al. (2018)*. In this paper, we focus on the results from
118 the intensive campaigns. We present measurements obtained at each site during the wet and dry
119 seasons of the studied periods: (i) PM size distribution and mass concentrations and (ii) PM
120 chemical composition including carbonaceous aerosol, water-soluble organic carbon, water-
121 soluble inorganic ions, dust and trace elements in different size fractions. Experimental method
122 including description of sites, types of measurements and analyses, meteorological conditions,
123 will be presented in the section 2, whereas results and discussion are discussed in the sections
124 3 and 4 of the paper, respectively.

125

2. Experimental method

2.1. Description of sites

Measurement campaigns have been performed in wet season (July 20-26, 2015 and July 4-13, 2016) and dry seasons (January 7-15, 2016 and January 5-14, 2017) at three sites in Abidjan (Côte d'Ivoire), representative of different sources, i.e. ADF for Abidjan Domestic Fires, AWB for Abidjan Waste Burning and AT for Abidjan Traffic (Figure 1), as well as one traffic site in Cotonou (Benin) (Figure 2).

As shown in Figure 3 which presents pictures of the different sampling sites, the ADF site (5° 19' 44 "N, 4° 06' 21" W) is situated on a platform, 5 m above ground level, in Yopougon Bracody district near a market (Figure 1). This geographical area is highly populated with various small commercial activities such as a fish and meat-smoking by women. There are also many formal and informal settlements, which mainly use wood and charcoal as a source of fuel for private and professional combustion activities. Other sources of concern contributing to the mix of pollutant emissions in the area include transportation-related emissions, biomass burning, garbage bins or small landfills and various other fugitive sources. The AT site (5° 21' 14" N, 4° 01' 04" W) is located in Adjamé, on the roof of « 220 pharmacie logement building », about 7 m above ground level and roughly 10 m away from the main road. This site, close to the Adjamé market and to a bus station, is highly affected by traffic (Gbaka, bus, taxi, woro-woro, private cars…). The AWB site (5° 21' 12" N, 3° 56' 16" W) is located at Akouédo in the district of Cocody, on the roof of « Talafiguié », a building 15 m above ground level. This site is close to the big waste burning area of Abidjan established since 1965, which covers an area of 153 ha. The Cotonou Traffic (CT) (6° 22' 19" N, 2° 26' 5" E) site is located in Cotonou, on the «Sogema» building roof, about 7 m above ground level. This site is close to the Dantokpa market and also to the biggest crossroad of Cotonou (intersection of 4 main roads). This site is highly influenced by intense traffic activities. As previously mentioned, such a site is interesting because the vehicle fleet and fuels are different in Cotonou compared to Abidjan: (1) there are many two-wheel vehicles in Cotonou whereas a few only in Abidjan; (2) in Cotonou, gasoline is of poor quality due to the illegal fuel transport from Nigeria and (3) the roads are in worse conditions in Cotonou than in Abidjan.

2.2. Measurements

During each intensive campaign, two 3-hour samples collected with cascade impactors operating in parallel are obtained for three consecutive days (i.e. six size-resolved samples per site during each campaign), to allow size-speciated characterization of the aerosol chemical composition. Note that the choice of the 3-hour periods is linked to the period of maximum pollution for each site (e.g. morning at ADF site, afternoon at AT site, morning at CT site). There is no specific period at AWB site since the activities are roughly the same during the day. The first impactor with 4 stages ($PM_{>2.5}$; $PM_{2.5-1}$; $PM_{1-0.2}$; $PM_{<0.2}$) includes 4 quartz fiber filters (QMA, Whatman) for mass and carbonaceous aerosol (EC, OC and WSOC analysis). The second impactor with 3 stages ($PM_{>2.5}$; $PM_{2.5-1}$; $PM1_{-0.1}$) is equipped with three Teflon filters (Zefluor, Pall Corporation®), dedicated for water-soluble ions species and trace elements. Due to operational problems in july 2016, this second 3-stage cascade impactor is replaced by another 3-stage cascade impactor with different size cuts ($PM_{>10}$, $PM_{10-2.5}$, $PM_{2.5-1}$). For consistency, results will be presented as an ultrafine (UF), fine (F) and coarse (C) classification. The two first stages ($PM_{>2.5}$ and $PM_{2.5-1}$) being considered as the coarse particulate fraction, the $PM_{1-0.1}$ or $PM_{1-0.2}$ stage, the fine particulate fraction and the $PM_{<0.2}$ stage, the ultrafine fraction. All the filters are prepared and analyzed at the Laboratoire d'Aerologie in Toulouse under different protocols described in the following paragraphs. Note that the quartz filters are prefired before sampling.

2.3. Analyses

2.3.1. Gravimetric analyses

Aerosol mass concentrations are obtained using a high-precision balance (SARTORIUS MC21S), placed under a controlled temperature and humidity atmosphere (Person and Tymen, 2005). Before weighing, the filters are kept 24 hours in the weighing room at an ambient relative humidity of 30 ±15%. The filters are weighed before and after sampling. Result of a gravimetric measurement consists of the average of 2 to 4 weighing whose differences do not exceed 5µg. The standard error on a gravimetric measurement is therefore less than 10 µg, typically representing less than 5% of the particles mass.

2.3.2. Carbonaceous aerosols

Carbonaceous aerosol is determined with thermal analysis with a two-step method adapted from Cachier et al. (1989). Two aliquots of the same filter are separately analyzed.

186   One portion is directly analyzed for its total carbon content (TC). The other portion is

187   first submitted to a pre-combustion step (2 h at 340°C under pure oxygen) in order to eliminate

188   Organic Carbon (OC), and then analyzed for its Elemental Carbon (EC) content. Organic

189   carbon (OC) concentrations are calculated as the differences between TC and EC. Note that the

190   aerosol carbon content is quantified by a non-dispersive infrared (NDIR) detector with G4

191   ICARUS instrument with a detection limit of the order of 2 $\mu gC.cm^{-2}$. Uncertainty is in the

192   order of 5% for TC, while being in the range of 5-20%, for EC and OC.

193   2.3.3 Water Soluble Organic Carbon analysis

194   WSOC measurements are performed using a total organic carbon analyzer (Sievers M9).

195   A detailed description of this technique is reported in Favez et al. (2008). Briefly, the full

196   oxidation of total organic carbon into CO_2 is obtained by coupling chemical oxidation (with

197   ammonium persulphate) and UV light. CO_2 is then quantified by conductivity. Analyses are

198   conducted on 20 ml of solution extracts. For UF samples, solutions to be analyzed are obtained

199   using a total filter surface of 3cm² (6x0.5 cm² punches symmetrically taken out of each QMA

200   filter), whereas, for C and F sizes, due to the geometry of the spots at the surface of the filters,

201   samples are divided into equivalent parts (1/2 or 1/4 of 47 mm filters, rest of the filters being

202   used for carbonaceous analysis). The extraction protocol consists of 16h soaking under soft

203   shaking in an Erlen-Meyer containing 20mL of ultra-pure water. Prior to WSOC analysis, water

204   extracts are filtered through Teflon (PTFE) filters (0.2μm pore size diameter) in order to remove

205   any suspended particle. Measurement uncertainty, given by the manufacturer, is of the order of

206   7%. The overall calculated blank value is of the order of $2.27 \pm 0.33 \, \mu gC.cm^{-2}$, which represents

207   16.4± 8.5% of the mean WSOC content. For each sample, duplicate analyses show a good

208   reproducibility.

209   2.3.4. Water-soluble ionic species

210   Water-soluble ionic species (Na^+, NH_4^+, K^+, Mg^{2+}, Ca^{2+}, SO_4^{2-}, NO_3^- and Cl^-) are

211   analyzed using ion chromatograph (IC), following the analytical protocol described in Adon et

212   al. (2010). Briefly, the aerosol water-soluble fraction is first extracted from half-sampled Teflon

213   filter (the other part being used for trace element analysis), with a 10-min sonication in plastic

214   vials including 6 ml or 10 ml of purified water with a controlled resistivity of 18.2MΩ. Then

215   these vials are subjected to ionic chromatograph analysis or stored at +4°C if not analyzed

216   immediately. Cations are analyzed with Dionex DX-100 and anions with Dionex DX-500 with

217 a detection limit of 1 to 6 ppb depending on ionic species. Uncertainties in the range of 1-50%

218 is found depending on ionic species.

219 ### 2.3.5. Trace elements

220 The protocol to measure trace element concentrations is developed and performed at the

221 Laboratory of Environmental Geosciences of Toulouse. Half-sampled Teflon filters (the other

222 part being used for water-soluble ionic species, see below) are mineralized by acid digestion

223 with a 10 ml concentrated HNO_3 and 0.5 ml HF solution (Lamaison, 2006) using a closed vessel

224 microwave accelerated reaction system (MARS 5, CEM Corporation) at high pressure (700 psi)

225 (Celo et al. 2010). The digestion is realized in 3 steps: a rise in temperature at 130°C in 3min

226 and holding for 1 min, then, a second rise at 160°C in 1 min and holding for 30 seconds and

227 finally a third rise to 180°C in 1 min and holding for 3min. After a 12 h cooling period, the

228 solutions are evaporated at 80°C, and concentrated in 7 ml of 2% concentrated HNO_3 solution,

229 before analysis by ICP-MS which are performed with a 7500 ce Agilent Technologies

230 instrument equipped with a collision cell, and using In and Re as internal standards. The

231 detection limit is less than 10 ppt. For all the samples, the final blank values and detection limit

232 on filters are taken into account for final concentrations calculations. 13 trace metals are

233 considered in this work: Al, Ti, Cr, Mn, Fe, Ni, Cu, Zn, Ba, La, Th, Pb and Cd.

234 ### 2.3.6. Dust calculation

235 Many methods can be used to quantify dust concentrations. We have selected three

236 methods (Sciare et al. 2005, Guinot et al. 2007, Terzi et al. 2010) to underline the uncertainties

237 linked to dust estimates.

238 (1) Sciare et al. (2005) method consists of using soluble calcium data obtained with Ionic

239 Chromatography (IC), to estimate the dust concentrations following the relationship:

240 dust = 10.96*nss-Ca^{2+}, where nss-Ca^{2+} (=1.02*Ca^{2+}-0.038*Na^+) refers to non-sea-salt

241 calcium concentration.

242 (2) Guinot et al. (2007) method is based on a chemical closure where fine and coarse

243 particle aerosols are separated in 4 components (EC, POM, WSI and dust). EC, WSI,

244 and total aerosol mass are directly experimentally determined (see below paragraphs).

245 POM concentrations are obtained from OC concentrations experimentally determined

246 and k, the OC/POM conversion factor. Dust concentrations are obtained from measured

247 Ca^{2+} concentrations and f, the abundance of calcium in dust. The k and f values are

248 obtained from a linear regression (L) between the reconstructed and the weighed aerosol

249   mass concentrations. Briefly, first step consists of focusing on the aerosol coarse

250   fraction. k is fixed to 1.8 and as a result of (L) just mentioned, f is obtained to be in the

251   range of 0.012 to 0.15 depending on our sites. Second step deals with the aerosol fine

252   fraction. The f values just obtained for the aerosol coarse fraction are applied to the fine

253   fraction and k ratios are estimated using (L) to be in the range of 1.2 to 2.1. Note that at

254   all of our sites, the correlation between Ca^{2+} and the missing mass between the weighed

255   and the reconstructed aerosol mass is sufficiently good (r^2=0.9) to support the

256   consistency of this simple approach for the evaluation of dust. Also, f and k values are

257   included in the range of values provided in the literature (He et al. 2001; Sun et al. 2004;

258   Guinot et al. 2007). However, it is important to mention that the range of f and k

259   coefficients are large which is due to the source mixing observed in this study.

260   (3) In Terzi et al. (2010) method, dust is obtained with the following relationship: dust =

261   1.89[Al] + 1.21[K] + 1.95[Ca] +1.66[Mg] + 1.7 [Ti] +2.14[Si] + 1.42[Fe]. In our study,

262   all these elements are determined except Silica (Si). Consequently, we used mean Si

263   values obtained from different relationships available in the literature (SiO_2 = 3*Al_2O_3

264   for Alastuey et al., 2005, Si = 4.0*Al for Zhang et al., 2003 and Si = 2.03*Al for

265   Chiapello et al., 1997).

266   The results of dust concentrations estimated from the three methodologies above described are

267   summarized in the Table 1 for wet season (WS) 2016 and dry season (DS) 2017. Indeed, Ca,

268   Al, and Fe concentrations measured by ICP-MS are only available in WS2016 and DS2017 due

269   to experimental problems, whereas Ca^{2+} concentrations measured by IC are available for all

270   campaigns. As shown in table 1, the dust obtained from Ca^{2+} measured by IC (Sciare et al.,

271   2005) and by the Guinot et al. (2007) method is lower than that obtained from trace elements

272   (Terzi et al., 2010) for DS2017 whereas in the same order of magnitude in WS2016. Such

273   results are in agreement with methodological aspects. Indeed, Al, Fe, Ca … obtained by ICP-

274   MS include both soluble and insoluble particles whereas Ca^{2+} measured by IC only include

275   soluble particles. During the dry season, comparison of Ca measured by ICP-MS (not shown

276   here) is higher than that of the IC, by a factor of 1.7, 1.8, 2.2 and 1.1, at the ADF, AWB, AT,

277   and CT sites respectively. By contrast, this factor is low and constant (1.3) in the wet season

278   for all the sites. In our study, due to the lack of trace element data for WS2015 and DS2016,

279   dust estimations are performed from Guinot et al. (2007) method. This choice globally implies

280   an underestimate of dust concentrations by a factor of 1.5 to 3.1 in DS2017.

281

282 **2.3.7. Aerosol chemical closure methodology**

283   As previously mentioned and detailed, aerosol chemical closure is performed following

284 the Guinot et al. (2007) methodology.

285

286   **2.4. Meteorological conditions**

287   In Figure 4, meteorological data (surface temperature, wind directions and speed) issued

288 from the NOAA Integrated Surface database (ISD; see https:// www.ncdc.noaa.gov/isd) and the

289 ASECNA (Agence pour la Sécurité de la Navigation Aérienne en Afrique et à Madagascar) are

290 presented for the South-West Africa region including Abidjan and Cotonou. As expected, this

291 area is under the influence of the Convergence Zone of two air masses of a different nature, i.e.

292 Harmattan (hot and dry continental trade winds) from the north and Monsoon (humid maritime

293 trade winds) from the south (Figure 4). Ground contact between these two air masses constitutes

294 the intertropical front (ITF) of which the fluctuations during the year determine the seasons in

295 the Gulf of Guinea (Tapsoba, 1997). During the dry season (from November to March),

296 temperatures are relatively high with maximum around 30°C on the coast. The humidity is low,

297 since the prevailing Harmattan wind blows from the desert, usually bringing dust (Figure 4,

298 lower line). The period from June to September, especially in July is the wet season period

299 when daytime temperatures are slightly lower, with maximum around 26/28°C on the coast

300 (Figure 4, upper line). At this season, the humidity level is high across the region. On the coast,

301 rains may occur from March to November.

302 During our campaigns (not shown here), temperatures are roughly the same at Abidjan and

303 Cotonou, reaching 28°C and 26°C in the dry and wet seasons, respectively. Gentle to moderate

304 wind speeds are observed during the measurement campaigns at the two cities, with average

305 values of 15-20 and 15-22 $km.h^{-1}$ at Abidjan and Cotonou, respectively. There is no

306 precipitation at CT site during the studied periods. In Abidjan on the contrary, low rains occur

307 both in wet and dry periods with cumulative precipitation higher in DS2017 (7mm), than in

308 WS2016 (4.7mm) and WS2015 (2mm). There is no rain in DS2016 (https://www.historique-

309 meteo.net/afrique/).

310   **2.5. Backward trajectories**

311   The Hybrid Single-Particle Lagrangian Integrated Trajectory (HYSPLIT) modelling

312 system (Air resources laboratory, Draxler and Rolph, 2012) is used for the trajectory analysis.

313 HYSPLIT model is run to compute 120 h back trajectories ending at Abidjan and Cotonou at

50 m a.g.l. (Figure 5). Global Data Assimilation System reanalysis database is used as meteorological input, with a 0.25×0.25 degrees horizontal resolution. Results presented in Figure 5, confirm that air masses mainly come from the north with a few from the south-west in January, whereas from the south-west and the south in July. Therefore, in January, Abidjan and Cotonou are mainly impacted by polluted air masses from surrounding areas and northern countries with possible dust and west African biomass burning influences, whereas in July, the impact of oceanic sources and of long-range south African biomass burning may be observed.

3. Results

3.1. Aerosol size distribution and mass concentration

In Figure 6, the relative mass distribution of PM for Coarse (C), Fine (F) and Ultra-Fine (UF) particle sizes in percentages are presented with bulk mass concentration averages indicated in the black boxes for each site and for each campaign. As it may be seen, bulk concentrations vary widely from site to site and from campaign to campaign. During the wet season, the average total concentrations range from 82 to 676 $\mu g.m^{-3}$ in 2015 and 56 to 358 $\mu g.m^{-3}$ in 2016, with the maximum at the Abidjan Domestic Fire (ADF) site. While during the dry season, values range from 168 to 269 $\mu g.m^{-3}$ in 2016 and from 114 to 559 $\mu g.m^{-3}$ in 2017, with maximum concentration obtained at the Cotonou Traffic (CT) and ADF sites. In terms of size distribution, concentration peaks may be observed for all aerosol size-fractions which are found to exhibit different seasonal patterns. UF particles (<0.2 µm) represent the highest contributor to the bulk mass at the ADF site, by up to 60 % (335.3 $\mu g.m^{-3}$) in DS2017. F particles (1-0.2 µm) are the second most important contributor and both combined particle sizes account for more than 85 % of the total mass at the ADF site. In this site, ultra-fine and fine fractions are also found to be maximum during WS2015 and WS2016 by up to 90 and 83%, respectively. Let us note that C particle contribution in bulk is relatively higher in the traffic and waste burning sites than in ADF site (40%) whereas F and UF particle contributions are on the order of 60%.

In terms of PM2.5, the results of this work are presented in Figure 7. The mass concentration of PM2.5 averaged over DS2016 and DS2017 are 154 ± 7, 144 ± 42, 134 ± 7 and 211 ± 51 $\mu g.m^{-3}$ at the ADF, AWB, AT and CT sites, respectively and 338 ± 24, 45 ± 3, 52 ± 4 and 70 ± 1 $\mu g.m^3$ over the wet seasons (2015-2016). The increase in PM2.5 is of the order

345   of 54% at ADF from dry to wet season, whereas a sharp reduction (more than 60%) is obtained

346   at AWB, AT, and CT sites.

347   **3.2. Carbonaceous aerosol**

348   **3.2.1. EC and OC concentrations**

349   In Figure 8, EC relative mass contributions are presented for each size, site and

350   campaign: wet season 2015 (WS2015), wet season 2016 (WS2016), dry season 2016 (DS2016)

351   and dry season 2017 (DS2017). Mean EC bulk mass concentrations are added in the black boxes

352   for each size and for each campaign. The most striking feature is that the ADF site

353   concentrations are higher than at the other sites in WS2016 and in DS2017, whereas of the same

354   order of CT site concentrations in the other seasons. Mean concentration at the CT site ($16\mu g.m^{-}$

355   ^{3}) is slightly higher than at the AT site ($10\mu g.m^{-3}$), whereas the lowest concentrations are found

356   at the AWB site. Results of the EC size distribution are very consistent among the different

357   sites (Figure 8). Whatever the site and the season, higher EC concentrations are found in C

358   (42%) and UF (43%) particles compared to F particles.

359   Same data are presented for OC concentrations in Figure 9. It may be underlined that

360   ADF OC values are always higher than in the other sites by a factor ranging from 6 to 30, for

361   all seasons and particle sizes, with highest and lowest values respectively in DS2017 and DS

362   2016. In terms of size distribution, maximum OC concentrations at the ADF site may be found

363   in UF (53%), then F (29%) and finally C (18%) particles. The same distribution is observed for

364   the traffic sites in DS2016, however, for the other campaigns, OC size distribution looks like

365   the EC ones with higher concentrations in UF and C particles than in F particles.

366   As shown in Figure 10, the highest OC/EC ratios are always obtained at the ADF site

367   with a value as high as 25 for F particles in WS2016 whereas the lowest values are found in

368   DS2017. This is the same feature for the other sites with ratios lower than 2 in DS2017. OC/EC

369   ratios in AWB site are higher than in the traffic sites. Note that values at AT site are higher than

370   CT values in the wet season whereas lower in the dry season. Finally, it is interesting to

371   underline that linear correlations between EC and OC are obtained in the ultrafine and fine

372   modes in all campaigns, particularly in DS2017 (r^{2} = 0.8, 0.8, 0.9 and 0.9) at the ADF, AWB,

373   AT and CT sites, respectively. This suggests that different studied sources can be assessed as

374   significant sources of both EC and OC.

375

3.2.2. Water-Soluble Organic Carbon

377   Concentrations of WSOC and WSOC/OC ratios are presented in Table 2 for each size

378   (UF, F, C and $PM_{2.5}$) and campaign. As seen, WSOC are always higher at the ADF site than in

379   other sites, at least by a factor of 12. Maximum values are obtained in WS2016 with an average

380   of 16.47, 17.08 and 79.68 $\mu gC.m^{-3}$ for coarse, fine and ultra-fine fractions, respectively,

381   followed by WS2015 and DS2017. WSOC concentrations are the lowest in DS2016, with an

382   average of 4.14, 6.95 and 21.89 $\mu g.m^{-3}$ for coarse, fine and ultrafine fractions, respectively. In

383   terms of seasonality, there is not a clear trend in WSOC values at the AWB and AT sites,

384   whereas at the CT and ADF sites, WSOC values are found to be respectively higher and lower

385   in dry seasons compared to wet seasons. It is also interesting to note that WSOC are maximum

386   in UF sizes in the AT, ADF and AWB sites. At the CT site, the highest values are found in the

387   coarse particulate fractions, except in DS2016.

388   As expected, WSOC is strongly correlated with OC (r=0.7 at ADF, 0.8 at AT, 0.5 at

389   AWB and 0.7 at CT), whereas correlations with EC are weaker, especially at the AWB and CT

390   sites with values ranging from 0.1 to 0.4, respectively. Finally, when looking at WSOC/OC

391   ratios (Table 2), maximum values are obtained at the ADF site with PM2.5 ratios as high as

392   43%, followed by the AT and AWB sites with 32%. The lowest value (23%) is found at the CT

393   site. Also, Table 2 shows that there is no clear seasonality in WSOC/OC values, excepted at

394   ADF where maximum values occur during the wet season. Note as for WSOC, that ratios are

395   maximum in UF and F fractions for all sites except at the CT site where the ratio for coarse

396   fraction is the highest.

3.3. Water-soluble ionic species

398   Figure 11 shows the relative contribution of the major ions to the total concentration

399   (also given) of the ions in the different particle modes (C and F) at the ADF, AWB, AT and CT

400   sites for the different measurement campaigns. Let us recall here that only C and F fractions

401   may be documented due to the our experimental protocol. Total concentrations present

402   maximum values in ADF and CT sites. Values in AWB and AT sites are of the same order of

403   magnitude and lower by a factor of 2 than in ADF and CT sites. The contribution of different

404   ions show significant variations from site to site. The dominant ionic species at the ADF site

405   over all campaigns is chloride (Cl^-), with a 26% contribution, followed by nitrate (NO_3^-) (16%),

406   calcium (Ca^{2+}) (13%) and potassium (K^{2+}) (12%). Sulfate (SO_4^{2-}), ammonium (NH_4^+), sodium

407 (Na$^+$) and to a lesser extent magnesium (Mg^{2+}) contributions are lower, ranging from 4 to 7%

408 of the total ion species. The lowest contribution is for organic acids with their total value lower

409 than 5%. NO$_3^-$ is the major ionic component at the AWB and AT sites, representing 24% and

410 29% of the total water soluble inorganic concentration, respectively. The second major

411 contributor in AWB and AT is SO$_4^{2-}$, accounting for 21% and 17% of the ion mass, respectively

412 followed by Ca^{2+} (12% and 15%) and Cl$^-$ (15% and 13%). In CT, Ca^{2+} is predominant with a

413 relative abundance of 24%, followed by NO$_3^-$ (23%), SO$_4^{2-}$ (19%) and Cl$^-$ (13%). Na$^+$, NH$_4^+$

414 and K$^+$ contributions are lower and in the same order of magnitude in AT, AWB and CT sites,

415 ranging from 4 to 9% of the total ion species. Note that organic gases contributions at AT, CT

416 and AWB is of the same order than in ADF, with lower values at CT. It is interesting to

417 underline in the Figure 11, that NO$_3^-$ contribution is always higher in the coarse than in the fine

418 size. Conversely, K$^+$ always higher in the fine than in the coarse size. In CT, Ca^{2+} in the fine

419 fraction is as high as in the coarse fraction whereas in AT, AWB and ADF, Ca^{2+} coarse fraction

420 is predominant. Fine particle contribution may be noticed for Cl$^-$ in ADF whereas in the other

421 sites, Cl$^-$ is most likely dominated by coarse particles. Finally, SO$_4^{2-}$ is mainly found in the fine

422 mode at the AT, AWB and CT sites, but in the coarse mode in ADF site.

423 In terms of seasonal variations, it may be shown in Figure 11 that higher Cl$^-$ values are found

424 in wet seasons than in the dry seasons everywhere, except in ADF site where there is no marked

425 difference between seasons. For example, the mean relative total percentages of Cl$^-$ at the CT

426 site are 38 and 24% in the WS2015 and WS2016, respectively, while these percentages decrease

427 significantly to 18 and 13% in the DS2016 and DS2017, respectively. The Cl$^-$/Na$^+$ ratios are

428 about 1.5 everywhere in both seasons, in agreement with the typical sea water ratio (1-1.2)

429 (Hara et al.,2004), except at the ADF site where these ratios increase to 4 and 5 in wet and dry

430 season, respectively and at the AWB site in the dry season (2). K$^+$ and Ca^{2+} are always higher

431 in dry season than in wet season except for Ca^{2+} in ADF where values are of the same order.

432 Finally, the same trend is observed for NO$_3^-$ and SO$_4^{2-}$ with higher values in dry than in wet

433 seasons at AWB and CT sites whereas values at ADF and AT sites are of the same order of

434 magnitude for the two seasons.

435 **3.4. Trace element concentrations**

436 Table 3 shows the mean values of the major trace elements in bulk aerosol at the

437 different studied sites in WS2016 and DS2017, with their corresponding relative abundances in

438 the total aerosol mass into brackets. Let us recall that data are not available in WS2015 and

439 DS2016. The concentrations of trace elements span a wide range, from 0.2 to 25.2 µg.m^{-3}.

440   Among the measured elements, Al, K, Na and Ca are the most abundant, followed by Fe and

441   Mg. In DS2017, Al and Na concentrations are higher in AWB than in the other sites. The

442   minimum value for these species is found in ADF site. Values in traffic sites are of the same

443   order of magnitude and higher than in ADF site. Maximum of Ca and K values may be found

444   in CT and ADF site respectively. It is interesting to note that Al, K, Na concentrations are higher

445   in the dry season than in the wet season. Such feature is less clear for Ca, whose seasonal

446   variability is less marked except in AWB and AT sites. In terms of Mg, maximum values are

447   observed in ADF site and of the same order of magnitude whatever the season. Fe abundance

448   is higher in AWB and CT sites than in ADF and AT sites and higher in DS2017 than in WS2016

449   everywhere. The other metals (Ti, P, Zr, Zn, Cr, Mn, Pb and Ni) represent less than 0.5% and

450   2% of the total mass in WS2016 and DS2017, respectively, at all sites, with Cr, Mn, Pb and Ni

451   exhibiting less seasonal variability compared to the rest of the metal elements.

452   To assess the relative contribution of crustal and non-crustal origin of elemental aerosol

453   loadings, source enrichment factor (EF) of a trace element X have been first calculated with the

454   following formula using both literature data of the typical elemental composition of the upper

455   continental crust (Mason and Moore, 1982; Taylor, 1964), measured elemental composition

456   from this study and Al as a reference element :

457

$$EF_X = \frac{\dfrac{[X]_{atm}}{[Al]_{atm}}}{[X]_{soil} \Big/ [Al]_{soil}}$$

458   Where $[X]_{atm}$ and $[Al]_{atm}$ are the concentrations of the chemical element X and Al in the

459   atmosphere, respectively, and $[X]_{soil}$ and $[Al]_{soil}$ are the typical concentrations of the element

460   X and Al in the earth's crust, respectively. Al is frequently used as a reference element assuming

461   that its anthropogenic sources in the atmosphere are negligible (Gao et al., 2002; Cao et al.,

462   2005; Xu et al., 2012). In all sampling sites, EF values typically lower than 5 are obtained for

463   several trace elements (Be, Sc, Ti, V, Fe, Ga, Sr, Nb, Rh, Ba, La, Ce, Pr, Nd, Sm, Eu, Gd, Tb,

464   Dy, Ho, Er, Tm, Yb, Lu, Ta, Th and U). This suggests a natural origin of these species (Freitas

465   et al., 2007; Gao et al., 2002). The most enriched elements (EF>100) are Sb, Sn, Zn, Se, Te,

466   Cd, Pb, Bi and Mo at nearly all of the sites, indicating significant anthropogenic origin (Wang

467   et al., 2006). These elements are mainly emitted into the atmosphere through fossil fuel

468   combustion, traffic emission, wear of brake lining materials and industrial processes (Watson

469   and Chow, 2001; Samara and al., 2003). Secondly, source contributions have been estimated

470   from these EF values following the method described by Arditsoglou and Samara (2005). Note

471   that this study refers to ratios for a limited list of sources, perhaps not including the African

472 source specificities. As a result, it may be seen that 30% of trace element concentrations is of

473 anthropogenic origin at ADF site whereas about 17 % at the others sites.

3.5. Dust

475 Figure 12 shows dust concentrations calculated from Guinot et al. (2007) methodology

476 (see paragraph 2.3.6) for C and F particle sizes at the different sites for each season. Note that

477 as for WSI and trace element and due to our sampling procedure, there are values for fine and

478 coarse particles for all seasons excepted for WS2016 with values for coarse particles only.

479 During the wet season, coarse dust concentrations range from 5 to 25 $\mu g.m^{-3}$ in 2015 and 9 to

480 37 $\mu g.m^{-3}$ in 2016, with higher values at the CT and ADF sites in 2015 and at AT, CT and ADF

481 in 2016. In WS2015, fine dust concentrations range from 12 to 49 with maximum values at

482 AFD and CT sites also. During the dry season, values range from 38 to 156 $\mu g.m^{-3}$ in 2016 and

483 from 41 to 116 $\mu g.m^{-3}$ in 2017, with maximum concentrations obtained at the CT site, followed

484 by AWB site. When considering mean values of the dry seasons, total dust at Cotonou traffic

485 (CT) is 2.4 times the values found at AT, 1.6 times at AWB and 3.4 times at ADF. Seasonal

486 comparison shows that total dust concentration is higher in the dry seasons than in WS2015 by

487 a factor of 3 in AT, 2.6 in CT and 4 in AWB, but of the same order of magnitude in ADF site.

3.6. Aerosol chemical closure

489 The aerosol chemical closure obtained using the Guinot et al. (2007) method (see below)

490 at the different sites for each season is presented in Figure 13. Results show clear intra- and

491 inter-annual variations at all of the sites, as well as significant differences among the sites. In

492 total, dust accounts for 39 to 75% of the bulk PM mass at both traffic sites, with no clear

493 seasonal cycle and higher contributions in Cotonou (Figures 13c and 13d). These percentages

494 vary from 32 to 64% at the AWB site, and from 18 to 35% at the ADF site, with percentages

495 1.8 times higher in the dry season than in the wet season in AWB and no clear seasonal

496 difference in ADF (Figures 13a and 13b). Carbonaceous aerosol, the sum of EC and POM,

497 show large contributions at the ADF site (from 49 to 69% of the total PM mass), with relatively

498 similar proportions in each season (Figure 13a). The absence of a clear seasonal pattern is also

499 observed in CT whereas carbonaceous aerosol is slightly higher in WS than in DS in AWB (23

500 and 16% respectively) and AT (37 and 21% respectively) (Figures 13b-d). Carbonaceous

501 aerosol contribution accounts for about 11- 49% of the total mass at both traffic sites with higher

502 values in AT (mean of 30%) than in CT (13%). The ion percentages in PM fractions present

503 the same pattern at AT, CT and AWB sites with higher values in wet than in dry seasons. In

504   these sites, we may notice that coarse particles are larger in the wet season whereas of the same

505   order of magnitude than fine particles in the dry seasons. In ADF, no marked difference may

506   be found between the seasons and the sizes (Figure 13).

507

4. Discussion

509   A discussion of the results site by site (Abidjan domestic fire site, traffic sites both together and

510   waste burning site) will be first proposed. We will scrutinize (1) the proximity between the sites

511   and the sources; (2) the source specificity with more or less incomplete combustion (e.g. wood

512   combustion and two-wheel vehicle emission factors are higher than gasoline emission factors

513   (Keita et al., 2018); (3) the relative influence of other local sources or transported sources to

514   the studied sites such as dust and biomass burning; (4) the occurrence of continental air masses;

515   (5) the variation of the boundary layer height (as reported by Colette et al., 2007); and (6) the

516   meteorological parameters (e.g. temperature, relative humidity and wet deposition) to explain

517   the differences of pollutant concentrations and their seasonal and inter-annual variabilities.

518   In a second part, we will present comparison of our values with other DACCIWA values and

519   also with literature values for other intensive campaigns in Africa.

520

4.1. Abidjan Domestic Fires (ADF)

522   As shown in the above paragraphs, maximum values are obtained at the ADF site, for aerosol

523   mass, EC, OC, WSOC, water-soluble ionic species (e.g. Cl^-, NO_3^-, Ca^{2+} and K^+) and some trace

524   elements such as Mg and K (whereas Al, Na and Fe are lower than in the other sites). Also,

525   aerosol $PM_{2.5}$ values are well above the annual and daily WHO guidelines of 25 and 10 $\mu g.m^{-3}$

526   respectively, whatever the season.

527   Such pattern is due to the proximity of the ADF site to the studied combustion source: in that

528   area, the use of wood combustion is very active due to commercial activities of women drying

529   fish and meat and domestic cooking. This is also confirmed by the high relative importance of

530   total carbon in aerosol mass whatever the size (49 to 69%) and by values of source enrichment

531   factor. Indeed, at least 30% of trace element concentrations are of anthropogenic origin at ADF

532   site. In addition, wood combustion is well known to be highly pollutant due to incomplete

533   combustion: this is shown here by the measurements of very high OC/EC ratios at ADF, on the

534   order of the one measured at the source level by Keita et al. (2018). This is also shown by

535   WSOC relative importance which is expected for wood burning following Yu et al. (2018),

536   Tang et al. (2016), Feng (2006) and Saxena and Hildemann (1996) and by the strong correlation

537   of WSOC with biomass burning K^+ tracer.

538   Chloride is most likely associated with sea salt origin (55% of total composition of the sea

539   water) or secondary aerosol production (Li et al., 2016). Its high concentration at the ADF site

540   remains lower than the typical concentration in sea-water suggesting a secondary production

541   source. The size distributions of Cl^-, K^+, NH_4^+ and SO_4^{2-} support the conclusion that the

542   predominance of these elements in fine particle mode at the ADF site could be associated with

543   anthropogenic emissions, particularly biomass combustion and domestic fires, or with

544   secondary inorganic aerosols origin. This is confirmed by Cl^-/Na^+ ratio values as shown earlier.

545   Contrarily, Ca^{2+} and NO_3^- contributions to the total ions at the ADF site peak mainly in the large

546   particle fraction and may be attributed to quasi natural origin, primarily to dust emissions and

547   nitrate formation by reaction processes, respectively. In addition, Na^+ and Mg^{2+} display similar

548   size distributions at the ADF site, with the major contribution in the coarse particle fraction,

549   suggesting the common sea salt origin of these two elements (Belis et al., 2013).

550   As we have shown above, the lower proportion of metal elements at the ADF site (6.5% of the

551   bulk concentration) can be explained by the less dominant influence of re-suspended dust

552   particles compared to traffic sources. Elements such as Cr, Mn, Pb and Ni have less seasonal

553   variability than other metallic elements. These small proportions of these non-crust elements

554   suggest a low contribution of elements emitted mainly by anthropogenic activities such as

555   industrial processes (Viana et al., 2007 and 2008; Minguillón et al., 2014). Finally, the Zn/Cd

556   ratio has been also examined. A value of 29 close to ratio reported for gasoline vehicle (27, Qin

557   et al., 1997) is obtained for the ADF site, indicating that this site is also impacted by traffic

558   sources.

559   High values of WSOC/OC ratios are expected to be harmful to health (Ramgolam et al., 2009,

560   Val et al., 2013). This effect is being enhanced by the particulate size measured at this site (Kim

561   et al., 2003; Wilson et al., 2002). Indeed, the relative mass distribution of PM and OC particle

562   sizes shows a major contribution of particles less than 1 µm (as high as 85% for PM). This

563   could be due to the fact that carbonaceous aerosols are formed near emission sources and are

564   mainly of submicron size (Boucher, 2012). Note that EC also presents large coarse particle

565   contribution.

566   In terms of seasonality, higher concentrations of aerosol mass, OC, WSOC, EC and total water

567   soluble ionic species (SO_4^{2-}, NH_4^+ and NO_3^-) are observed in WS2015 and WS2016 than in

568   DS2016. This may be explained by a more incomplete combustion in the wet seasons than in

569   DS2016 due to the use of moist wood for cooking and smoking fish, which leads to large

amount of smoke and higher particulate emission factor values. Note that DS2017 values are as important as the ones of wet seasons, which will be explained later in the text. With regard to WSOC, their variabilities may be also linked to meteorological factors, such as solar radiation (Tang et al., 2016; Favez et al., 2008) and relative humidity (Liang et al., 2016). At ADF site, temperatures are roughly similar in both seasons. However, RH variability may play a role since it is higher in wet season than in dry season. Finally, our results indicate no clear seasonal cycle for Cl^-, which confirms its anthropogenic origin, as previously shown.

4.2. Traffic sites (Abidjan traffic and Cotonou Traffic sites)

Let us recall first that the two traffic sites have been chosen since they are representative of the traffic diversity in West Africa. At CT site, both personal cars, taxis and an important two-wheel fleet may be found whereas at AT site, there are buses, taxis and personal cars. Also, the distance between the site and the traffic sources is the same for the two traffic sites, slightly larger than the distance between the site and the wood burning sources at ADF site.

In these two sites, concentrations are high with $PM_{2.5}$ values well above the WHO guidelines. Average aerosol mass, EC, OC, dust and water soluble ionic concentrations (with NO_3^- and Ca^{2+} maximum at AT and CT sites respectively) are higher at CT than at AT site by a factor of 1.5 to 2. Note that this poor air quality found in Cotonou has been reported by Cachon et al. (2014). The higher values found in Cotonou could be due to more intense traffic in Cotonou than in Abidjan. Also in Cotonou, this traffic is associated with the lack of public transportation and the use of highly polluted mopeds (aged over 15 years) (Gounougbe, 1999; Avogbe et al., 2011), despite the effort in the last 10 years to restrict their use. Several studies such as MMEH (2002) have shown that more than 94,000 mopeds and 350,000 second-hand vehicles are in circulation in Cotonou. Other factors contributing to the local pollution include outdoor restaurants using charcoal and motorcycle garages, which are more present around the Cotonou traffic site compared to Abidjan site. It also includes anthropogenic dust. Indeed, at Cotonou, the lack of road infrastructure favours the resuspention of dust particles. Finally, other sources may potentially influence aerosol seasonal composition in these two sites, including marine aerosols, transported dust and biomass burning particles as well as anthropogenic aerosols from the surrounding countries (Figure 5). Note also that source enrichment factor values show that about 17% of trace element concentrations are of anthropogenic origin at both traffic sites and that the relative importance of total carbon in mass is higher at AT than at CT sites. As a consequence, aerosol mass, composition and size depend on the season and the two traffic sites are differently affected.

604 The EC and OC concentrations measured in both traffic sites, are higher in dry than in wet

605 season. Such variations may be explained by several factors: particulate wet deposition

606 occurring during the wet season, reduction of traffic flow due to school vacations and

607 meteorological influence. Higher EC concentrations are obtained at CT than at AT sites at both

608 seasons. Similar pattern is observed for OC in dry season. In contrast, lower values are obtained

609 at CT than at AT sites in wet season. Differences between OC values in wet season between

610 the two sites can be due to the influence of long-range transport of biomass burning aerosols

611 coming from Southern Africa, which could be more important in Abidjan than in Cotonou, as

612 shown by the backtrajectory patterns given in Figure 5. On the contrary, in the dry season,

613 higher OC values at Cotonou may be explained by local sources as already detailed, but also

614 by surrounding sources such as Nigerian anthropogenic and biomass burning sources (Figure

615 5).

616 In terms of WSOC concentrations, concentrations at the AT site are on average higher than

617 those recorded at the CT site in the wet season, but lower in dry season. The presence of dust

618 can produce semi-volatile organic gas scavenging and therefore WSOC and OC enhancement.

619 Such a phenomenon can explain the highest WSOC concentrations observed in dry season at

620 the CT site where dust concentrations are highest (see dust paragraph). Moreover, this can also

621 explain why the maximum WSOC are in coarse particles at CT, while at AT maximum values

622 are in ultra-fine particles.

623 Total WSI concentrations are larger at AT site in the wet than in the dry season with higher

624 values in coarse particles. At CT site, total WSI concentrations in fine particles are higher in

625 the dry than in the wet season whereas same values are obtained in coarse particles for both

626 seasons. Note that CT values are generally higher than AT values with a more important

627 contribution of fine particles in the dry season. These WSI variations can be explained by the

628 relative importance of Ca^{2+}, SO_4^{2-} and NO_3^- in both sites.

629 First, Ca^{2+} contribution to total WSI is higher in CT site than in AT site with no clear seasonal

630 variation at CT site and higher values in dry season than in wet season at AT site. Also at CT,

631 fine and coarse Ca^{2+} particles are in the same range, whereas coarse Ca^{2+} particles are

632 predominant at AT site. Such feature may be explained by the impact of dust sources including

633 long-range dust transport at Abidjan and a combination of long-range dust transport and road

634 resuspension at Cotonou.

635 Second, the relative contribution of SO_4^{2-}, NH_4^+ and NO_3^- as a percentage of total WSI in the

636 different particle modes is reduced in the wet season. During the wet season, the clean winds

637 surrounding the ocean before reaching the measurement sites could contribute to lower the

proportion of these species, in addition to the scavenging processes during the rainy days. Unlike the wet season, a relatively good correlation of 0.87 (SO_4^{2-} versus NH_4^+), 0.73 (NO_3^- versus NH_4^+) and 0.87 (SO_4^{2-} versus NO_3^-) has been found in coarse particles, indicating similar sources for these three species during the dry season. In order to try to identify these sources, the ratio of SO_4^{2-}/Ca^{2+} and NO_3^-/Ca^{2+} has been determined. The average SO_4^{2-}/Ca^{2+} and NO_3/Ca^{2+} ratios in combined coarse particles (1.07 and 2.58 during the wet season and 0.33 and 1.60 during the dry season) are higher than the corresponding ratios for typical soil (0.026 and 0.003, respectively). On the other hand, the SO_4^{2-}/Ca^{2+} ratio increases in the fine particles (5.07 during the wet season and 2.53 during the dry season), while that of NO_3^-/Ca^{2+} remains almost constant (2.86 during the wet season and 1.65 during the dry season). This implies that the atmosphere at AT and CT sites is enriched by SO_4^{2-} formed as anthropogenic secondary particles, possibly from sulfur containing pollution sources (Seinfield and Pandis, 1998), particularly in fine particle mode, and by NO_3^- mostly coming from nitrogen containing sources in all particle sizes. The higher contributions of these elements during the dry season could result from a combination of several factors: 1) an atmosphere loaded with dust favoring heterogeneous chemistry to obtain secondary aerosol and the rise of biomass burning emissions; 2) the increase of photochemical activity and higher concentrations of hydroxyl radicals in the dry season, which can oxidize SO_2 from combustion (Arndt et al., 1997) to SO_4^{2-} (Li et al., 2014) ; and 3) the wind transport of anthropogenic secondary particles from the industrial zone located upstream from our sites. Finally, the proportion of Cl^- relative to the total mass of ions is highest for coarse particles at both traffic sites especially during the wet season, suggesting that Cl^- at AT and CT sites if from natural origin and probably from sea salt emissions.

If we focus now on dust during the two wet seasons, concentrations are higher in 2016 than in 2015 at CT and AT sites for coarse particles (no data of fine particles are available in WS2016). This is consistent with observed aerosol optical depth (AOD) values at CT, which increased by a factor of 2 between 2015 and 2016. No AOD value is given by Léon et al. (2019) at Abidjan in WS2015 to allow such comparison in Abidjan. Moreover, during the wet season, an Angström coefficient (AE) on the order of 1 has been found at CT site, indicating smaller particles that could be due to road resuspension. It is interesting to note that during WS2016, AOD and AE are respectively higher and lower at Abidjan than at Cotonou. Again, this is consistent with our dust concentrations at CT site. In Abidjan, we could assume that another source of Ca^{2+}, which is not taken into account in our dust calculations, may explain our dust concentration data. That may be the result of anthropogenic Ca^{2+} emissions from residential

671 combustion, more important in 2016 than in 2015 as shown earlier
672 (http://naei.beis.gov.uk/overview/pollutants?pollutant_id=84).

673 The relative contribution of dust generally peaks in the coarse mode and, to a lesser extent, in
674 the fine mode, reflecting their natural origin. It is interesting to note that the dust contribution
675 observed in this study for the year 2016 at the Abidjan site is in agreement with the results of
676 Xu et al. (2019) which show a $PM_{2.5}$ dust contribution of 35-50% compared to our values of
677 18-52%.

678

679 **4.3. Abidjan Waste Burning site**

680 Concentrations measured at AWB site are slightly lower than values found in the other sites.
681 This could be explained by the distance of the site to the studied source (here waste burning
682 source) which is more important than in the other sites. However, $PM_{2.5}$ values are also higher
683 than WHO guidelines.

684 Aerosol mass, EC and OC concentrations are higher in dry than in wet season, which suggests
685 less waste burning activities during the wet season or impacts of other local anthropogenic
686 sources or long-range biomass burning sources. Highest values are found in DS2017 with the
687 lowest OC/EC ratio, as at AT site. OC/EC ratio is highly variable at AWB (1-10) which
688 confirms that AWB site may be impacted by different types of sources as well as by secondary
689 aerosol organic formation which can be detected for OC/EC higher than 2 (Turpin et al. 1990;
690 Hildermann et al. 1991; Chow et al. 1996). Note that OC/EC typical for waste burning source
691 is of the order of 8 (Keita et al., 2018).

692 It is also observed that at the AWB site, PM mass concentrations are mainly distributed in C
693 mode (30-44%) over the entire period of study, excepted during the WS2015, and to a lesser
694 extend in F mode (21-44%). EC and OC being mainly distributed in C and UF modes. Water-
695 soluble fraction of organic carbon is important (32%) and on the order of the one found at AT
696 site. Same for WSI concentrations and WSI composition. At AWB, WSI values are globally
697 slightly higher in wet than in dry season. However, it is interesting to underline that Ca^{2+} is
698 much higher in dry season than in wet season, especially in DS2017. This is in agreement with
699 dust concentrations and trace element concentrations, which have been found to be maximum
700 at AWB, reaching 35.8% of the total PM mass in the dry season. These maximum percentages
701 are due to the large contribution of both Al and Na crustal elements which account for about
702 26%. Also note that Cu/Sb of 0.08 in DS2017, which indicate an influence of re-suspended
703 particles. A Zn/Cd value of 56 is obtained for the AWB site which is in close agreement with

704 values reported for oil burning (Watson et al., 2001, Samara et al., 2003). That could indicate

705 that oil might be one of the waste burning materials.

706 Our result suggests that AWB aerosol mass is influenced by a mix of sources, including fuel

707 combustion and mineral salt from sources around the measurement site, associated to long-

708 range source impact of dust and biomass burning which will be further discussed in the next

709 paragraph.

710

711 **4.4. Interannual variability of aerosols in Abidjan and Cotonou**

712 EC and OC concentrations are generally higher in DS2017 than in DS2016 for all the sites. This

713 is not due to the meteorological condition, which is similar in both years. This is also not due

714 to biomass burning impacts. Indeed, when looking at MODIS burnt areas for our period of study

715 (http://www.aeris-data.fr/redirect/MODIS-MCD64A1), burnt areas of west African savannas

716 are higher in 2016 than in 2017. Therefore, carbonaceous aerosol concentrations should be

717 higher in 2016. Then, this could be due to a counter effect between biomass burning emission

718 strength and air mass transport efficiency. As a result, biomass burning impact could not explain

719 the difference in EC and OC during the dry season between 2016 and 2017. Rather, this is due

720 to the variability of local sources. In DS2016 in Abidjan, there was a general strike of civil

721 servants of the State with important consequences on urban activities. Lower activities were

722 observed (lower fish smoking emissions, lower traffic ..) in DS2016 compared to DS2017, thus

723 explaining the lower EC and OC concentrations at Abidjan sites. In Cotonou, highest

724 carbonaceous aerosol values in DS2017 may be explained by backtrajectory patterns: Cotonou

725 would be impacted by air masses coming from the high polluted Lagos (Nigeria) area in that

726 period whereas from less polluted northern areas in DS2016. Such an assumption is validated

727 by the AOD values at 550nm from MODIS satellite images (http://www.aeris-

728 data.fr/redirect/MODIS-MCD64A1), which show very high particulate concentrations in the

729 Guinean Golf (Figure 14).

730 This figure also shows the AOD difference between Cotonou and Abidjan for DS2017, with

731 higher values at Cotonou than in Abidjan for the campaign period, in agreement with our

732 measurements of aerosol mass, EC, OC and dust. This is confirmed by the DACCIWA

733 sunphotometer AOD and Angström coefficient (AE) measurements at Abidjan and Cotonou

734 (Léon et al., 2019; Djossou et al., 2018). Indeed, in DS2017, during our period of

735 measurements, mean AOD in Cotonou is of the order of 1.3 versus 0.9 in Abidjan for an AE of

736 0.6 for both sites, which clearly indicates the presence of coarse dust particles.

Finally, aerosol mass and dust concentrations have been seen to be higher in DS2016 than in DS2017 in Abidjan whereas values are on the same order of magnitude at Cotonou. Such high values at Abidjan in DS2016 can be explained by the back-trajectory pattern with air-masses all coming from northern dusty areas in DS2016 (Bodélé depression in Tchad, Prospero et al. (2002), Washington et al., (2003), Knippertz et al. (2011), Balarabe et al., (2016)) and/or from northern dusty countries (Mali, Niger) (Ozer, 2005), whereas in DS2017, contribution of southern marine clean air-masses may also be noted.

In the wet season, aerosol mass, EC and OC are higher in WS2015 than in WS2016. This may be due to particulate wet deposition, more efficient in WS2016 which have been seen earlier to be more rainy (4.7mm) than in WS2015 (2mm). Moreover, at AT site, dust concentrations are higher for coarse particles in WS2016 than in WS2015. Such variations may be explained by long-range dust sources and/or road dust resuspension processes. As no dust event has been noticed, local source explanation seems to be more evident.

Finally, in AT, CT and AWB, OC/EC ratios are globally on the same order for WS2015, WS2016 and DS2016, with values similar to that of gasoline emissions or old diesel vehicles. However, the ratios are lower for DS2017, with values typical of those of diesel emission (Mmari et al., 2013; Keita et al., 2018). The general strike occurring in DS2016 in Abidjan could explain such a difference. Indeed, more EC emissions occurred in DS2017 than in DS2016 for constant OC emissions. This can be the result of more diesel traffic. Similar ratio values have also been previously reported for other megacities such as Agra in India with 6.7 (Pachauri et al., 2013), Helsinki in Finland with 2.7 (Viidanoja, 2002), Cairo in Egypt with 2.9 (Favez, 2008), Paris in France with 3.5 (Favez, 2008), and Milan in Italy with 6.6 (Lonati et al., 2007).

4.5. Comparison with DACCIWA and literature measurements

Firstly, the comparison between our data and other DACCIWA results including other time sampling focuses on PM$_{2.5}$ levels, since these particle sizes are relevant for health impact studies (Xing et al., 2016). In addition to our values, Figure 7 presents data from Xu et al. (2019) using personal samplers collected in the same area and at the same dates in 2016 during 12h on women at the ADF site, students at the AWB site and drivers at the CT site, and from Djossou et al. (2018) study based on weekly measurements collected at the same areas and for the same periods as this study. We note that PM$_{2.5}$ directly measured on women are 2.3 and 0.9 times our values obtained at the ADF site in dry and wet seasons, respectively, and 3.4 and 4.9 times higher on students than at the AWB site, and 1.6 and 2.1 times higher on drivers than at the CT

site. Also, our values are on average 1.6, 3, 5 and 8 times higher than weekly values of Djossou et al. (2018) including our 3 days of measurements at the AWB, ADF, AT and CT sites respectively. As it may be seen, the lowest concentrations are observed in Djossou et al. (2018), whereas the highest concentrations are recorded in Xu. et al. (2019). This is valid for all sites, seasons and campaigns. Differences between our values and Djossou values may be explained by the sampling times of the two studies. Indeed, Djossou measurements are weekly, taking into account diurnal activities during all the week, including week-end and nights which have expected lower $PM_{2.5}$ concentrations. Our study includes only maximum pollution conditions for each site. The highest differences occur for the traffic sites. This may be clearly understood since diurnal and weekly variations of traffic sources are the most variable. Comparison between our values and Xu et al. (2019) values is also interesting. Indeed, it is at the ADF site that on-site and women $PM_{2.5}$ concentrations are the closest, which shows that this site is the most representative of the pollution exposure to women. The biggest differences are found at the AWB site. As already mentioned, distance from the site to the waste burning source is more important than for other sites, which explains why student concentrations are much higher than on-site concentrations. At the Cotonou traffic site, measurements taken from people are also higher than on site measurements. Such differences can be explained by additional pollution exposure as people move around. Note that the sampling technique may also play a role in such a comparison. In terms of seasonal variation, our results are in agreement with long-term EC measurements conducted by Djossou et al. (2018) for the same sites and period. Finally, Table 4 compares our $PM_{2.5}$ results to literature data for different traffic sites in the world including the same daily sampling time. It is interesting to note that our values are situated at the higher end of the range of $PM_{2.5}$ data observed from the other sites.

Secondly, Table 5 compares our OC and EC values to those obtained by Djossou et al. (2018) and Xu et al. (2019) as previously described for the same period and the same sites. It is interesting to note that Djossou's values are in general lower than ours. Indeed, for the wet and dry seasons, our OC measurements are 4 and 1.4 times higher than Djoussou's at the AT site, 2.1 and 5.7 times higher at the CT site, and 2.5 and 2.5 times higher at the ADF site, respectively. As for $PM_{2.5}$, this can be explained by the different sampling times between our experiments that were performed at the peak of urban activities, while Djossou's dataset represents weekly integrated values. Differences at the ADF site are largely explained by the temporal pattern of fish smoking activities which take place every day, only in the morning, as such the associated pollution is not well represented in the weekly sampling. Finally, there are less differences at the AWB site between both datasets since waste burning emissions occur

805 night and day throughout the week. Comparisons made between our values and those of Xu's

806 personal data show that both OC and EC are of the same order at the ADF site, whereas Xu

807 values are higher than ours at the CT and AWB sites. This result is in agreement with what we

808 found with $PM_{2.5}$ concentrations as detailed above. Finally, Table 6 presents OC and EC for the

809 $PM_{2.5}$ comparison between our values and other recent studies dealing with traffic sites in other

810 regions of the world and with similar operational conditions. We find that our values are situated

811 in the middle of the range observed in these different studies. Briefly, as presented in Table 7,

812 it is interesting to compare our WSOC concentrations to literature data for different traffic sites

813 of the world. We note that our values are on the same order as values found in Asia and higher

814 than those found in Europe.

815 Thirdly, the percentages of the total WSI to PM mass (15-20%) at the three Abidjan sites (ADF,

816 AWB and AT) are in the same order of magnitude than the data from $PM_{2.5}$ personal exposure

817 samples collected at the same locations in 2016 by Xu et al. (2019). Our results also are very

818 close to the ionic contribution of 9% of the PM_{10} mass found at the urban curbside site in Dar

819 es Salaam in Tanzania during the wet season 2005 by Mkoma (2008).

820

821 **5. Conclusion**

822 This paper presents the mass and the size-speciated chemical composition of particulate matter

823 (PM) during the dry and wet seasons in 2015, 2016 and 2017. Measurements were performed

824 at three sites in Abidjan, representative of domestic fire (ADF), waste burning (AWB) and

825 traffic (AT) sources, and at one traffic site in Cotonou (CT).

826 It is important to underline that our results and their temporal variations are very sensitive to

827 (1) the source activities whose pollution levels are highly linked to socio-economic status of

828 each city; (2) the impact of imported pollution (sea-salt, biomass burning, dust, anthropogenic

829 emissions from neighboring countries), according to air mass origins; and (3) the particle wet

830 deposition.

831 The comparison between our results and literature data underlines the importance of the

832 distance of the chosen site to the sources. At the source level (such as ADF), pollution results

833 at the site are in agreement with exposure of people living at this site. However, at the other

834 sites, comparison is more difficult since the sites are under the influence of a mix of transported

835 sources. That shows the key importance of exposure studies to estimate air quality and health

836 impacts.

837 The main striking feature is that $PM_{2.5}$ values are well above the annual and daily WHO

838 guidelines of 25 and 10 $\mu g.m^{-3}$, respectively, whatever the site and the season. Also, measured

concentrations from this study are situated in the middle to the high part of the range of worldwide urban aerosol concentrations. In addition, we have stressed the importance of ultra-fine and fine particles in the studied aerosol and of species such as particulate organic matter and water soluble organic carbon, which are well known to be particularly harmful. This is again a warning signal for pollution levels in African capitals if nothing is done to reduce emissions in the future.

Our study constitutes an original database to characterize urban air pollution from specific African combustion sources. The next step will be to cross such an exhaustive aerosol chemical characterization to biological data in order to evaluate the impact of aerosol size and chemical composition on aerosol inflammatory properties.

Acknowledgements. The research leading to these results has received funding from the European Union 7th Framework Programme (FP7/2007-2013) under Grant Agreement no. 603502 (EU project DACCIWA: Dynamics-aerosol-chemistry-cloud interactions in West Africa). The authors greatly thank all the colleagues and operators who contribute to sampling during the different campaigns.

Author Contributions

J.A. and C.L. conceived and designed the study. J.A., C.L. and E.T.D. contributed to the literature search, data analysis/interpretation and manuscript writing. J.A., C.L., A.B. and E.T.D. contributed to manuscript revision. J.A., C.L., J.F.L, H.C, V.Y., A.A, C.G, C.Z, E.C and S.K. carried out the particulate samples collection and chemical experiments, analyzed the experimental data.

Additional Information

Figure S1 and Appendix A-D accompany this manuscript can be found in SupplementaryInformation.

Competing financial interests

The authors declare no competing financial interests

References

Adon, M., Galy-Lacaux, C., Yoboué, V., Delon, C., Lacaux, J. P., Castera, P., Gardrat, E., Pienaar, J., Al Ourabi, H., Laouali, D., Diop, B., Sigha-Nkamdjou, L., Akpo, A., Tathy, J. P., Lavenu, F. and Mougin, E.: Long term measurements of sulfur dioxide, nitrogen dioxide, ammonia, nitric acid and ozone in Africa using passive samplers, Atmos. Chem. Phys., 10(15), 7467-7487, doi:10.5194/acp-10-7467-2010, 2010.

Alastuey, A., Querol, X., Castillo, S., Escudero, M., Avila, A., Cuevas, E., Torres, C., Romero, P., Exposito, F. and Garcia, O.: Characterisation of TSP and PM$_{2.5}$ at Izaña and Sta. Cruz de Tenerife (Canary Islands, Spain) during a Saharan Dust Episode (July 2002), Atmospheric Environment, 39(26), 4715-4728, doi: 10.1016/j.atmosenv.2005.04.018, 2005.

Arditsoglou, A. and Samara, C.: Levels of total suspended particulate matter and major trace elements in Kosovo: a source identification and apportionment study, Chemosphere, 59(5), 669-678, doi: 10.1016/j.chemosphere.2004.10.056, 2005.

Arndt, R. L., Carmichael, G. R., Streets, D. G. and Bhatti, N.: Sulfur dioxide emissions and sectorial contributions to sulfur deposition in Asia, Atmospheric Environment, 31(10), 1553-1572, doi: 10.1016/S1352-2310(96)00236-1, 1997.

Avogbe, P. H., Ayi-Fanou, L., Cachon, B., Chabi, N., Debende, A., Dewaele, D., Aissi, F., Cazier, F. and Sanni, A.: Hematological changes among Beninese motor-bike taxi drivers exposed to benzene by urban air pollution, African Journal of Environmental Science and Technology, 5(7), 464-472, 2011.

Balarabe, M., Abdullah, K. and Nawawi, M.: Seasonal Variations of Aerosol Optical Properties and Identification of Different Aerosol Types Based on AERONET Data over Sub-Sahara West-Africa, ACS, 06(01), 13-28, doi:10.4236/acs.2016.61002, 2016.

Belis, C. A., Karagulian, F., Larsen, B. R. and Hopke, P. K.: Critical review and meta-analysis of ambient particulate matter source apportionment using receptor models in Europe, Atmospheric Environment, 69, 94-108, doi: 10.1016/j.atmosenv.2012.11.009, 2013.

Bisht, D.S., Dumka, U.C., Kaskaoutis, D.G., Pipal, A.S., Srivastava, A. K., Soni, V.K., Attri, S.D., Sateesh, M., Tiwari, S.: Carbonaceous aerosols and pollutants over Delhi urban environment: Temporal evolution, source apportionment and radiative forcing, Science of the Total Environment, 521-522: 431-445, 2015.

Bouhila, Z., Mouzai, M., Azli, T., Nedjar, A., Mazouzi, C., Zergoug, Z., Boukhadra, D., Chegrouche, S. and Lounici, H.: Investigation of aerosol trace element concentrations nearby Algiers for environmental monitoring using instrumental neutron activation analysis, Atmospheric Research, 166, 49-59, doi: 10.1016/j.atmosres.2015.06.013, 2015.

Cachier, H., Brémond, M.-P. and Buat-Ménard, P.: Carbonaceous aerosols from different tropical biomass burning sources, Nature, 340(6232), 371-373, doi:10.1038/340371a0, 1989.

Cachon, B. F., Firmin, S., Verdin, A., Ayi-Fanou, L., Billet, S., Cazier, F., Martin, P. J., Aissi, F., Courcot, D., Sanni, A. and Shirali, P.: Proinflammatory effects and oxidative stress within human bronchial epithelial cells exposed to atmospheric particulate matter ($PM_{2.5}$ and $PM_{>2.5}$) collected from Cotonou, Benin, Environmental Pollution, 185, 340-351, doi: 10.1016/j.envpol.2013.10.026, 2014.

Cao, J.J., Lee, S.C., Zhang, X.Y., Chow, J.C., An, Z.S., Ho, K.F., Watson, J.G., Fung, K., Wang, Y.Q. and Shen, Z.X.: Characterization of airborne carbonate over a site near Asian dust source regions during spring 2002 and its climatic and environmental significance, J. Geophys. Res., 110(D3), D03203, doi: 10.1029/2004JD005244, 2005.

Cassee, F. R., Héroux, M.-E., Gerlofs-Nijland, M. E. and Kelly, F. J.: Particulate matter beyond mass: recent health evidence on the role of fractions, chemical constituents and sources of emission, Inhalation Toxicology, 25(14), 802–812, doi:10.3109/08958378.2013.850127, 2013.

Celo, V., Dabek-Zlotorzynska, E., Mathieu, D., Okonskaia, I.: Validation of simple microwave-assisted acid digestion method using microvessels for analysis of trace elements in atmospheric $PM_{2.5}$ in monitoring and fingerprinting studies, The Open Chemical & Biomedical Methods Journal 3., 141-150, 2010.

Cesari, D., Donateo, A., Conte, M., Merico, E., Giangreco, A., Giangreco, F. and Contini, D.: An inter-comparison of $PM_{2.5}$ at urban and urban background sites: Chemical characterization and source apportionment, Atmospheric Research, 174-175, 106-119, doi: 10.1016/j.atmosres.2016.02.004, 2016.

Cheng, Z., Jiang, J., Chen, C., Gao, J., Wang, S., Watson, J. G., Wang, H., Deng, J., Wang, B., Zhou, M., Chow, J. C., Pitchford, M. L. and Hao, J.: Estimation of Aerosol Mass Scattering Efficiencies under High Mass Loading: Case Study for the Megacity of Shanghai, China, Environ. Sci. Technol., 49(2), 831-838, doi: 10.1021/es504567q, 2015.

Chiapello, I., Bergametti, G., Chatenet, B., Bousquet, P., Dulac, F. and Soares, E. S.: Origins of African dust transported over the northeastern tropical Atlantic, J. Geophys. Res., 102(D12), 13701-13709, doi: 10.1029/97JD00259, 1997.

Chow, J. C., Watson, J. G., Lu, Z., Lowenthal, D. H., Frazier, C. A., Solomon, P. A., Thuillier, R. H. and Magliano, K.: Descriptive analysis of $PM_{2.5}$ and PM_{10} at regionally representative locations during SJVAQS/AUSPEX, Atmospheric Environment, 30(12), 2079-2112, doi:10.1016/1352-2310(95)00402-5, 1996.

Colbeck, I., Nasir, Z. A., Ahmad, S. and Ali, Z.: Exposure to PM_{10}, $PM_{2.5}$, PM_1 and Carbon Monoxide on Roads in Lahore, Pakistan, Aerosol Air Qual. Res., 11(6), 689-695, doi:10.4209/aaqr.2010.10.0087, 2011.

Colette, A., Menut, L., Haeffelin, M. and Morille, Y.: Impact of the transport of aerosols from the free troposphere towards the boundary layer on the air quality in the Paris area, Atmospheric Environment, 42(2), 390-402, doi: 10.1016/j.atmosenv.2007.09.044, 2007.

948 Dieme, D., Cabral-Ndior, M., Garçon, G., Verdin, A., Billet, S., Cazier, F., Courcot, D., Diouf,
949   A. and Shirali, P.: Relationship between physicochemical characterization and toxicity of
950   fine particulate matter (PM$_{2.5}$) collected in Dakar city (Senegal), Environmental Research,
951   113, 1-13, doi:10.1016/j.envres.2011.11.009, 2012.

952 Ding, A., Huang, X. and Fu, C.: Air Pollution and Weather Interaction in East Asia, Oxford
953   Research Encyclopedias-Environmental Sience, doi:
954   10.1093/acrefore/9780199389414.013. 536, 2017.

955 Djossou, J., Léon, J.-F., Akpo, A. B., Liousse, C., Yoboué, V., Bedou, M., Bodjrenou, M.,
956   Chiron, C., Galy-Lacaux, C., Gardrat, E., Abbey, M., Keita, S., Bahino, J., Touré
957   N'Datchoh, E., Ossohou, M. and Awanou, C. N.: Mass concentration, optical depth and
958   carbon composition of particulate matter in the major southern West African cities of
959   Cotonou (Benin) and Abidjan (Côte d'Ivoire), Atmos. Chem. Phys., 18(9), 6275-6291,
960   doi:10.5194/acp-18-6275-2018, 2018.

961 Doumbia, E.H.T., Liousse, C., Galy-Lacaux, C., Ndiaye, S.A., Diop, B., Ouafo, M., et al. Real
962   time black carbon measurements in West and Central Africa urban sites. Atmospheric
963   Environment. 2012;54(0):529-37.

964 Draxler, R. R., and G. D. Rolph: Evaluation of the Transfer Coefficient Matrix (TCM) approach
965   to model the atmospheric radionuclide air concentrations from Fukushima, J. Geophys.
966   Res., 117, D05107, doi:10.1029/2011JD017205, 2012.

967 Du, Z., He, K., Cheng, Y., Duan, F., Ma, Y., Liu, J., Zhang, X., Zheng, M. and Weber, R.: A
968   yearlong study of water-soluble organic carbon in Beijing I: Sources and its primary vs.
969   secondary nature, Atmospheric Environment, 92, 514-521,
970   doi:10.1016/j.atmosenv.2014.04. 060, 2014.

971 Favez, O.: Caractérisation physico-chimique de la pollution particulaire dans des mégapoles
972   contrastées, Thèse de l'Université PARIS.DIDEROT (Paris 7), France, 2008.

973 Favez, O., Sciare, J., Cachier, H., Alfaro, S. C. and Abdelwahab, M. M.: Significant formation
974   of water-insoluble secondary organic aerosols in semi-arid urban environment, Geophys.
975   Res. Lett., 35(15), L15801, doi:10.1029/2008GL034446, 2008.

976 Feng, J., Guo, Z., Chan, C. K. and Fang, M.: Properties of organic matter in PM$_{2.5}$ at Changdao
977   Island, China - A rural site in the transport path of the Asian continental outflow,
978   Atmospheric Environment, 41(9), 1924-1935, doi: 10.1016/j.atmosenv.2006.10.064, 2007.

979 Feng, J., Hu, M., Chan, C. K., Lau, P. S., Fang, M., He, L. and Tang, X.: A comparative study
980   of the organic matter in PM$_{2.5}$ from three Chinese megacities in three different climatic
981   zones, Atmospheric Environment, 40(21), 3983-3994, doi:
982   10.1016/j.atmosenv.2006.02.017, 2006.

983 Freitas, M.C., Pacheco, A.M.G., Baptista, M.S., Dionísio, I., Vasconcelos, M.T.S.D. and
984   Cabral, J.P.: Response of exposed detached lichens to atmospheric elemental deposition,
985   Proc. ECOpole., 1(1/2), 15-21, 2007.

Gaga, E. O., Arı, A., Akyol, N., Üzmez, Ö. Ö., Kara, M., Chow, J. C., Watson, J. G., Özel, E., Döğeroğlu, T. and Odabasi, M.: Determination of real-world emission factors of trace metals, EC, OC, BTEX, and semivolatile organic compounds (PAHs, PCBs and PCNs) in a rural tunnel in Bilecik, Turkey, Science of The Total Environment, 643, 1285-1296, doi: 10.1016/j.scitotenv.2018.06.227, 2018.

Gao, Y., Nelson, E. D., Field, M. P., Ding, Q., Li, H., Sherrell, R. M., Gigliotti, C. L., Van Ry, D. A., Glenn, T. R. and Eisenreich, S. J.: Characterization of atmospheric trace elements on $PM_{2.5}$ particulate matter over the New York–New Jersey harbor estuary, Atmospheric Environment, 36(6), 1077–1086, doi:10.1016/S1352-2310(01)00381-8, 2002.

Genga, A., Ielpo, P., Siciliano, T. and Siciliano, M.: Carbonaceous particles and aerosol mass closure in $PM_{2.5}$ collected in a port city, Atmospheric Research, 183, 245-254, doi: 10.1016/j.atmosres.2016.08.022, 2017.

Gounougbe, F.: Pollution atmosphérique par les gaz d'échappement et état de santé des conducteurs de taxi-moto (Zemidjan) de Cotonou (Bénin), Thèse de doctorat en Médecine (832), 1999.

Guinot, B., Cachier, H. and Oikonomou, K.: Geochemical perspectives from a new aerosol chemical mass closure, Atmos. Chem. Phys., 7(6), 1657-1670, doi: 10.5194/acp-7-1657-2007, 2007.

Guttikunda, S. K. and Calori, G.: A GIS based emissions inventory at 1 km $\times$ 1 km spatial resolution for air pollution analysis in Delhi, India, Atmospheric Environment, 67, 101-111, doi:10.1016/j.atmosenv.2012.10.040, 2013.

Hara, K., Osada, K., Kido, M., Hayashi, M., Matsunaga, K., Iwasaka, Y., Yamanouchi, T., Hashida, G. and Fukatsu, T.: Chemistry of sea-salt particles and inorganic halogen species in Antarctic regions: Compositional differences between coastal and inland stations, J. Geophys. Res., 109, D20208, doi:10.1029/2004JD004713, 2004.

He, K., Yang, F., Ma, Y., Zhang, Q., Yao, X., Chan, C. K., Cadle, S., Chan, T. and Mulawa, P.: The characteristics of PM2.5 in Beijing, China, Atmospheric Environment, 35(29), 4959-4970, doi: 10.1016/S1352-2310(01)00301-6, 2001.

Hildemann, L. M., Markowski, G. R. and Cass, G. R.: Chemical composition of emissions from urban sources of fine organic aerosol, Environ. Sci. Technol., 25(4), 744-759, doi: 10.1021/es00016a021, 1991.

Huang, H., Ho, K. F., Lee, S. C., Tsang, P. K., Ho, S. S. H., Zou, C. W., Zou, S. C., Cao, J. J. and Xu, H. M.: Characteristics of carbonaceous aerosol in PM2.5: Pearl Delta River Region, China, Atmospheric Research, 104-105, 227-236, doi: 10.1016/j.atmosres.2011.10.016, 2012.

Jaffrezo, J.-L., Aymoz, G., Delaval, C., and Cozic, J.: Seasonal variations of the Water Soluble Organic Carbon mass fraction of aerosol in two valleys of the French Alps, Atmos. Chem. Phys., 5, 2809-2821, 2005.

1024 Keita, S., Liousse, C., Yoboué, V., Dominutti, P., Guinot, B., Assamoi, E.-M., Borbon, A.,
1025   Haslett, S. L., Bouvier, L., Colomb, A., Coe, H., Akpo, A., Adon, J., Bahino, J., Doumbia,
1026   M., Djossou, J., Galy-Lacaux, C., Gardrat, E., Gnamien, S., Léon, J. F., Ossohou, M.,
1027   N'Datchoh, E. T. and Roblou, L.: Particle and VOC emission factor
1028   measurements for anthropogenic sources in West Africa, Atmos. Chem. Phys., 18(10),
1029   7691-7708, doi:10.5194/acp-18-7691-2018, 2018.

1030 Khan, Md. F., Shirasuna, Y., Hirano, K. and Masunaga, S.: Characterization of $PM_{2.5}$, $PM_{2.5-10}$
1031   and $PM_{>10}$ in ambient air, Yokohama, Japan, Atmospheric Research, 96(1), 159-172,
1032   doi:10.1016/j.atmosres.2009.12.009, 2010.

1033 Kim, H., Liu, X., Kobayashi, T., Kohyama, T., Wen, F.-Q., Romberger, D. J., Conner, H.,
1034   Gilmour, P. S., Donaldson, K., MacNee, W. and Rennard, S. I.: Ultrafine Carbon Black
1035   Particles Inhibit Human Lung Fibroblast-Mediated Collagen Gel Contraction, Am J Respir.
1036   Cell. Mol. Biol., 28(1), 111-121, doi:10.1165/rcmb.4796, 2003.

1037 Knippertz, P., Tesche, M., Heinold, B., Kandler, K., Toledano, C. and Esselborn, M.: Dust
1038   mobilization and aerosol transport from West Africa to Cape Verde - a meteorological
1039   overview of SAMUM-2, Tellus B: Chemical and Physical Meteorology, 63(4), 430-447,
1040   doi:10.1111/j.1600-0889.2011. 00544.x, 2011.

1041 Kouassi, K. S., Billet, S., Garçon, G., Verdin, A., Diouf, A., Cazier, F., Djaman, J., Courcot,
1042   D. and Shirali, P.: Oxidative damage induced in A549 cells by physically and chemically
1043   characterized air particulate matter ($PM_{2.5}$) collected in Abidjan, Côte d'Ivoire, J. Appl.
1044   Toxicol., doi:10.1002/jat.1496, 2009.

1045 Lamaison, L. : Caractérisation des particules atmosphériques et identification de leurs sources
1046   dans une atmosphère urbaine sous influence industrielle, Thèse Doctorat, Univ des
1047   Sciences et Technologies, Lille, 2006.

1048 Léon, J.F., Akpo, A., Bedou, M., Djossou, J., Bodjrenou, M., Yoboué, V., et Liousse, C.:
1049   Profondeur optique des aérosols sur le sud de l'Afrique de l'Ouest, soumis à ACPD, 2019.

1050 Li, T.-C., Yuan, C.-S., Hung, C.-H., Lin, H.-Y., Huang, H.-C. and Lee, C.-L.: Chemical
1051   Characteristics of Marine Fine Aerosols over Sea and at Offshore Islands during Three
1052   Cruise Sampling Campaigns in the Taiwan Strait-Sea Salts and Anthropogenic Particles,
1053   Atmos. Chem. Phys. Discuss., 1-27, doi:10.5194/acp-2016-384, 2016.

1054 Li, Y., Schwandner, F. M., Sewell, H. J., Zivkovich, A., Tigges, M., Raja, S., Holcomb, S.,
1055   Molenar, J. V., Sherman, L., Archuleta, C., Lee, T. and Collett, J. L.: Observations of
1056   ammonia, nitric acid and fine particles in a rural gas production region, Atmospheric
1057   Environment, 83, 80-89, doi:10.1016/j.atmosenv.2013.10.007, 2014.

1058 Liang, L., Engling, G., Du, Z., Cheng, Y., Duan, F., Liu, X. and He, K.: Seasonal variations and
1059   source estimation of saccharides in atmospheric particulate matter in Beijing, China,
1060   Chemosphere, 150, 365-377, 2016.

1061 Liousse, C., Assamoi, E., Criqui, P., Granier, C., Rosset, R.: Explosive growth in African
1062   combustion emissions from 2005 to 2030, Environ. Res. Lett., 9, 035003, 2014.

Lonati, G., Ozgen, S. and Giugliano, M.: Primary and secondary carbonaceous species in $PM_{2.5}$ samples in Milan (Italy), Atmospheric Environment, 41(22), 4599-4610, doi:10.1016/j.atmosenv.2007.03.046, 2007.

Lowenthal, D., Zielinska, B., Samburova, V., Collins, D., Taylor, N. and Kumar, N.: Evaluation of assumptions for estimating chemical light extinction at U.S. national parks, Journal of the Air & Waste Management Association, 65(3), 249-260, doi:10.1080/10962247.2014.986307, 2015.

Mason, B., Moore, B.C.: Principles of Geochemistry, fourth ed. John Wiley and Sons, New York, pp. 46-47, 1982.

Minguillón, M. C., Cirach, M., Hoek, G., Brunekreef, B., Tsai, M., de Hoogh, K., Jedynska, A., Kooter, I. M., Nieuwenhuijsen, M. and Querol, X.: Spatial variability of trace elements and sources for improved exposure assessment in Barcelona, Atmospheric Environment, 89, 268-281, doi: 10.1016/j.atmosenv.2014.02.047, 2014.

Mkoma, S. L.: Physico-Chemical characterisation of atmospheric aerosols in Tanzania, with emphasis on the carbonaceous aerosol components and on chemical mass closure, PhD, Ghent University, Ghent, Belguim, 2008.

Mmari, A. G., Potgieter-Vermaak, S. S., Bencs, L., McCrindle, R. I. and Van Grieken, R.: Elemental and ionic components of atmospheric aerosols and associated gaseous pollutants in and near Dar es Salaam, Tanzania, Atmospheric Environment, 77, 51-61, doi: 10.1016/j.atmosenv.2013.04.061, 2013.

MMEH (Ministère des Mines de l'Energie et d'Hydraulique): Tableau de bord de l'Energie 2002 au Bénin, Direction Générale de l'Energie, 2002.

Ngo, N. S., Asseko, S. V. J., Ebanega, M. O., Allo'o Allo'o, S. M. and Hystad, P.: The relationship among $PM_{2.5}$, traffic emissions, and socioeconomic status: Evidence from Gabon using low-cost, portable air quality monitors, Transportation Research Part D: Transport and Environment, 68, 2-9, doi: 10.1016/j.trd.2018.01.029, 2019.

Ozer, P.: Estimation de la pollution particulaire naturelle de l'air en 2003 à Niamey (Niger) à partir de données de visibilité horizontale, 2005.

Pachauri, T., Singla, V., Satsangi, A., Lakhani, A. and Kumari, K. M.: Characterization of carbonaceous aerosols with special reference to episodic events at Agra, India, Atmospheric Research, 128, 98-110, doi: 10.1016/j.atmosres.2013.03.010, 2013.

Park, J. H., Mudunkotuwa, I. A., Mines, L. W. D., Anthony, T. R., Grassian, V. H. and Peters, T. M.: A Granular Bed for Use in a Nanoparticle Respiratory Deposition Sampler, Aerosol Science and Technology, 49(3), 179-187, doi:10.1080/02786826.2015.1013521, 2015.

Person, A. and Tymen, G.: Mesurage des particules en suspension dans l'air en relation avec la santé. Pollution atmosphèrique, 271-285, 2005.

1099 Pipal, A. S., Jan, R., Satsangi, P. G., Tiwari, S. and Taneja, A.: Study of Surface Morphology,
1100   Elemental Composition and Origin of Atmospheric Aerosols ($PM_{2.5}$ and PM_{10}) over Agra,
1101   India, Aerosol Air Qual. Res., 14(6), 1685-1700, doi:10.4209/aaqr.2014.01.0017, 2014.

1102 Pipal, A. S., Singh, S. and Satsangi, G. P.: Study on bulk to single particle analysis of
1103   atmospheric aerosols at urban region, Urban Climate, 27, 243-258, doi:
1104   10.1016/j.uclim.2018.12.008, 2019.

1105 Prospero, J.M., Ginoux, P., Torres, O., Nicholson, S.E., Gill, T.E.: Environmental
1106   characterization of global sources of atmospheric soil dust identified with the NIMBUS 7
1107   Total Ozone Mapping Spectrometer (TOMS) absorbing aerosol product, Rev. Geophys.,
1108   40, 2-1-31, 2002.

1109 Qin, Y., Chan, C. K. and Chan, L. Y.: Characteristics of chemical compositions of atmospheric
1110   aerosols in Hong Kong: spatial and seasonal distributions, Science of The Total
1111   Environment, 206(1), 25-37, doi: 10.1016/S0048-9697(97)00214-3, 1997.

1112 Ramgolam K, Favez O, Cachier H, Gaudichet A, Marano F, Martinon L, Baeza-Squiban
1113   A: Size-partitioning of an urban aerosol to identify particle determinants involved in the
1114   proinflammatory response induced in airway epithelial cells. Part Fibre
1115   Toxicol 2009, 6: 10. 10.1186/1743-8977-6-10.

1116 Rengarajan, R., Sudheer, A. K. and Sarin, M. M.: Aerosol acidity and secondary organic aerosol
1117   formation during wintertime over urban environment in western India, Atmospheric
1118   Environment, 45(11), 1940-1945, doi: 10.1016/j.atmosenv.2011.01.026, 2011.

1119 Samara, C., Kouimtzis, T., Tsitouridou, R., Kanias, G. and Simeonov, V.: Chemical mass
1120   balance source apportionment of PM_{10} in an industrialized urban area of Northern Greece,
1121   Atmospheric Environment, 37(1), 41-54, doi:10.1016/S1352-2310(02)00772-0, 2003.

1122 Satsangi, A., Pachauri, T., Singla, V., Lakhani, A. and Kumari, K. M.: Organic and elemental
1123   carbon aerosols at a suburban site, Atmospheric Research, 113, 13-21, doi:
1124   10.1016/j.atmosres.2012.04.012, 2012.

1125 Saxena, P., and Hildemann, L.M.: Water-soluble organics in atmospheric particles: a critical
1126   review of the literature and application of thermodynamics to identify candidate
1127   compounds, J. Atmos. Chem., 24(1), 57-109, 1996.

1128 Sciare, J., Oikonomou, K., Cachier, H., Mihalopoulos, N., Andreae, M. O., Maenhaut, W. and
1129   Sarda-Estève, R.: Aerosol mass closure and reconstruction of the light scattering
1130   coefficient over the Eastern Mediterranean Sea during the MINOS campaign, Atmos.
1131   Chem. Phys., 5(8), 2253-2265, doi:10.5194/acp-5-2253-2005, 2005.

1132 Seinfeld, J. H. and Pandis, S. N.: Atmospheric Chemistry and Physics: from Air
1133   Pollution to Climate Change, John Wiley and Sons, Inc. New York, 1998.

1134 Shahsavani, A., Naddafi, K., Jaafarzadeh Haghighifard, N., Mesdaghinia, A., Yunesian, M.,
1135   Nabizadeh, R., Arhami, M., Yarahmadi, M., Sowlat, M. H., Ghani, M., Jonidi Jafari, A.,
1136   Alimohamadi, M., Motevalian, S. A. and Soleimani, Z.: Characterization of ionic

composition of TSP and PM$_{10}$ during the Middle Eastern Dust (MED) storms in Ahvaz, Iran, Environ Monit Assess, 184(11), 6683-6692, doi:10.1007/s10661-011-2451-6, 2012.

Stone, R. S., Herber, A., Vitale, V., Mazzola, M., Lupi, A., Schnell, R. C., Dutton, E. G., Liu, P. S. K., Li, S.-M., Dethloff, K., Lampert, A., Ritter, C., Stock, M., Neuber, R. and Maturilli, M.: A three-dimensional characterization of Arctic aerosols from airborne Sun photometer observations: PAM-ARCMIP, April 2009, J. Geophys. Res., 115(D13), D13203, doi: 10.1029/2009JD013605, 2010.

Sullivan, A. P., Weber, R. J., Clements, A. L., Turner, J. R., Bae, M. S. and Schauer, J. J.: A method for on-line measurement of water-soluble organic carbon in ambient aerosol particles: Results from an urban site: on-line measurement of WSOC in aerosols, Geophys. Res. Lett., 31(13), doi: 10.1029/2004GL019681, 2004.

Sun, Y., Zhuang, G., Wang, Y., Han, L., Guo, J., Dan, M., Zhang, W., Wang, Z. and Hao, Z.: The airborne particulate pollution in Beijing - concentration, composition, distribution and sources, Atmospheric Environment, 38(35), 5991-6004, doi: 10.1016/j.atmosenv.2004.07.009, 2004.

Tang, X., Zhang, X., Ci, Z., Guo, J. and Wang, J.: Speciation of the major inorganic salts in atmospheric aerosols of Beijing, China: Measurements and comparison with model, Atmospheric Environment, 133, 123-134, doi: 10.1016/j.atmosenv.2016.03.013, 2016.

Tapsoba, D. : Caractérisation événementielle des régimes pluviométriques ouestafricains et de leur récent changement, Thèse de Doctorat, Univ.Paris-XI (Orsay). 100p, 1997.

Taylor, S. R.: Abundance of chemical elements in the continental crust: a new table, Geochimica et Cosmochimica Acta, 28(8), 1273-1285, doi: 10.1016/0016-7037(64)90129-2, 1964.

Terzi, E., Argyropoulos, G., Bougatioti, A., Mihalopoulos, N., Nikolaou, K. and Samara, C.: Chemical composition and mass closure of ambient PM$_{10}$ at urban sites, Atmospheric Environment, 44(18), 2231-2239, doi: 10.1016/j.atmosenv.2010.02.019, 2010.

Tunno, B., Longley, I., Somervell, E., Edwards, S., Olivares, G., Gray, S., Cambal, L., Chubb, L., Roper, C., Coulson, G. and Clougherty, J. E.: Separating spatial patterns in pollution attributable to woodsmoke and other sources, during daytime and nighttime hours, in Christchurch, New Zealand, Environmental Research, 171, 228-238, doi: 10.1016/j.envres.2019.01.033, 2019.

Turpin, B. J., Cary, R. A. and Huntzicker, J. J.: An In Situ, Time-Resolved Analyzer for Aerosol Organic and Elemental Carbon, Aerosol Science and Technology, 12(1), 161-171, doi:10.1080/02786829008959336, 1990.

Val, S., Liousse, C., Doumbia, E. H. T., Galy-Lacaux, C., Cachier, H., Marchand, N., Badel, A., Gardrat, E., Sylvestre, A. and Baeza-Squiban, A.: Physico-chemical characterization of African urban aerosols (Bamako in Mali and Dakar in Senegal) and their toxic effects in human bronchial epithelial cells: description of a worrying situation, Part Fibre Toxicol, 10(1), 10, doi:10.1186/1743-8977-10-10, 2013.

Viana, M., López, J. M., Querol, X., Alastuey, A., García-Gacio, D., Blanco-Heras, G., López-Mahía, P., Piñeiro-Iglesias, M., Sanz, M. J., Sanz, F., Chi, X. and Maenhaut, W.: Tracers and impact of open burning of rice straw residues on PM in Eastern Spain, Atmospheric Environment, 42(8), 1941-1957, doi: 10.1016/j.atmosenv.2007.11.012, 2008.

Viana, M., Maenhaut, W., ten Brink, H. M., Chi, X., Weijers, E., Querol, X., Alastuey, A., Mikuška, P. and Večeřa, Z.: Comparative analysis of organic and elemental carbon concentrations in carbonaceous aerosols in three European cities, Atmospheric Environment, 41(28), 5972-5983, doi: 10.1016/j.atmosenv.2007.03.035, 2007.

Viidanoja, J., Sillanpää, M., Laakia, J., Kerminen, V.-M., Hillamo, R., Aarnio, P. and Koskentalo, T.: Organic and black carbon in $PM_{2.5}$ and PM_{10}: 1 year of data from an urban site in Helsinki, Finland, Atmospheric Environment, 36(19), 3183-3193, doi: 10.1016/S1352-2310(02)00205-4, 2002.

Wang, X., Bi, X., Sheng, G. and Fu, J.: Chemical Composition and Sources of PM_{10} and $PM_{2.5}$ Aerosols in Guangzhou, China, Environ Monit Assess, 119(1-3), 425-439, doi: 10.1007/s10661-005-9034-3, 2006.

Washington, R., Todd, M., Middleton, N. J. and Goudie, A. S.: Dust-Storm Source Areas Determined by the Total Ozone Monitoring Spectrometer and Surface Observations, Annals of the Association of American Geographers, 93(2), 297-313, doi:10.1111/1467-8306.9302003, 2003.

Watson, J. G. and Chow, J. C.: Estimating middle-, neighborhood-, and urban-scale contributions to elemental carbon in Mexico City with a rapid response aethalometer, J. Air Waste Manag. Assoc., 51(11), 1522-1528, 2001.

Watson, J. G., Chow, J. C. and Houck, J. E.: $PM_{2.5}$ chemical source profiles for vehicle exhaust, vegetative burning, geological material, and coal burning in Northwestern Colorado during 1995, Chemosphere, 43(8), 1141-1151, doi:10.1016/S0045-6535(00)00171-5, 2001.

WHO (World Health Organization), 7 million premature deaths annually linked to air pollution. Media Centre news release. Geneva: World Health Organization. (http: //www.who.int/ mediacentre/news/releases/2014/airpollution/en/, 2014.

Wilson, M. R., Lightbody, J. H., Donaldson, K., Sales, J. and Stone, V.: Interactions between ultrafine particles and transition metals in vivo and in vitro, Toxicol. Appl. Pharmacol., 184(3), 172-179, 2002.

Xiang, P., Zhou, X., Duan, J., Tan, J., He, K., Yuan, C., Ma, Y. and Zhang, Y.: Chemical characteristics of water-soluble organic compounds (WSOC) in $PM_{2.5}$ in Beijing, China: 2011-2012, Atmospheric Research, 183, 104-112, doi: 10.1016/j.atmosres.2016.08.020, 2017.

Xie, Y., Wang, Y., Bilal, M. and Dong, W.: Mapping daily $PM_{2.5}$ at 500 m resolution over Beijing with improved hazy day performance, Science of The Total Environment, 659, 410-418, doi: 10.1016/j.scitotenv.2018.12.365, 2019.

Xu, H., Léon, J.-F., Liousse, C., Guinot, B., Yoboué, V., Akpo, A. B., Adon, J., Ho, K. F., Ho, S. S. H., Li, L., Gardrat, E., Shen, Z. and Cao, J.: Personal exposure to $PM_{2.5}$ emitted from typical anthropogenic sources in Southern West Africa (SWA): Chemical characteristics and associated health risks, Atmos. Chem. Phys. Discuss., 1-68, doi:10.5194/acp-2018-1060, 2019.

Xu, J., Zhang, Y., Zheng, S. and He, Y.: Aerosol effects on ozone concentrations in Beijing: a model sensitivity study, J Environ Sci (China), 24(4), 645-656, 2012.

Yu, P., Froyd, K. D., Portmann, R. W., Toon, O. B., Freitas, S. R., Bardeen, C. G., Katich, J. M., Schwarz, J. P., Williamson, C., Kupc, A., Brock, C., Liu, S., Gao, R.-S., Schill, G., Fan, T., Rosenlof, K. H., and Murphy, D. M.: An improved treatment of aerosol convective transport and removal in a chemistry-climate model, Geophys. Res. Lett., submitted, 2018.

Zghaid, M., Noack, Y., Bounakla, M., and Benyaich, F.: Pollution atmosphérique particulaire dans la ville de Kenitra (Maroc), Pollution atmosphérique [En ligne], N° 203, mis à jour le 12/10/2015, URL : http://lodel.irevues.inist.fr/pollution-atmospherique/index.php?id=1184, https://doi.org/10.4267/pollution-atmospherique.1184

Zhang, X. Y., Gong, S. L., Shen, Z. X., Mei, F. M., Xi, X. X., Liu, L.C., Zhou, Z. J., Wang, D., Wang, Y. Q., and Cheng, Y.: Characterization of soil dust aerosol in China and its transport and distribution during 2001 ACE-Asia: 1. Network observations, J. Geophys. Res. Atmos., 108(D9), 4261, doi:10.1029/2002JD002632, 2003.

1248 **Figure caption**

1249 Figure 1: Map of the city of Abidjan reporting the geographical location of DACCIWA urban
1250   sampling sites.

1251 Figure 2: Map of the city of Cotonou reporting the geographical location of DACCIWA urban
1252   sampling site.

1253 Figure 3: Pictures of the different sampling sites : (a) Traffic in Cotonou (Benin, CT station),
1254   (b) Waste burning in Abidjan (Côte d'Ivoire, AWB station), (c), Domestic fire, showing
1255   smoking activity in Yopougon, Abidjan (Côte d'Ivoire, ADF station), (d) '' woro-woro
1256   and Gbaka '' traffic in Abidjan (Côte d'Ivoire, AT station).

1257 Figure 4: Wind, pressure and temperature diagram at Abidjan and Cotonou during the different
1258   campaigns.

1259 Figure 5: Back trajectories arriving at Abidjan (a) and Cotonou (b) for each season (WS2015,
1260   WS2016, DS2016 and DS2017).

1261 Figure 6: Aerosol Mass concentrations at the different study sites for each campaign and for the
1262   different sizes (C in black, Fine in light Grey, Ultra-fine in grey). Bulk aerosol mass is
1263   indicated in boxes.

1264 Figure 7: Comparison of PM 2.5 mass concentrations in $\mu g.m^{-3}$ at the four sites with those
1265   obtained by Djossou et al. (2018) and Xu et al. (2019) for the same site and period.

1266 Figure 8: EC relative concentrations in each size classes (C in black, Fine in light grey, Ultra-
1267   fine in grey) at the different study sites for each campaign. Bulk EC concentration for
1268   each site is indicated in boxes.

1269 Figure 9: OC relative concentrations in each size classes (C in black, Fine in light grey, Ultra-
1270   fine in grey) at the different study sites for each campaign. Bulk OC concentration for
1271   each site is indicated in boxes.

1272 Figure 10: OC/ EC ratio for the different campaigns and sites for each aerosol size (C in black,
1273   Fine in light grey, Ultra-fine in grey). Each box shows the median and the first and the
1274   third quartiles.

1275 Figure 11: Water-soluble ionic species speciation for each site, each campaign and each aerosol
1276   size.

1277 Figure 12: Dust concentrations at the different study sites for each campaign and for the
1278 different sizes (C in black, Fine in light grey, Ultra-fine in grey).

1279 Figure 13: Size-speciated aerosol chemical composition for each site, for each campaign and
1280 each aerosol size.

1281 Figure 14: MODIS Aerosol optical depth regional distribution over West Africa. Data are for
1282 2017, focusing on our campaign date at Abidjan (a-c 01/11-12-left part) and Cotonou
1283 (b-d 01/6-7, right part).

1284

1285

1286

1287

1288

1289

1290

1291
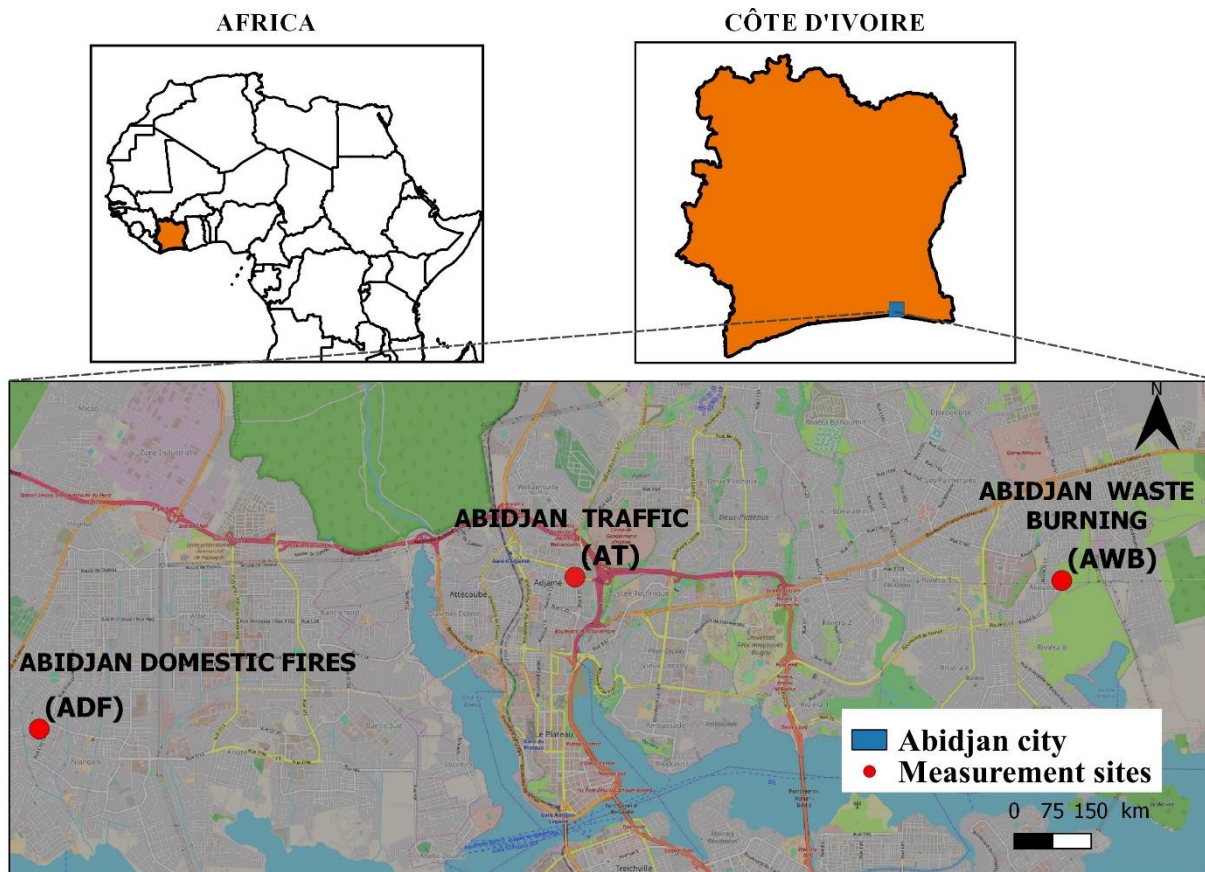
1292

1293

1294   Figure1

1295

1296

1297

1298
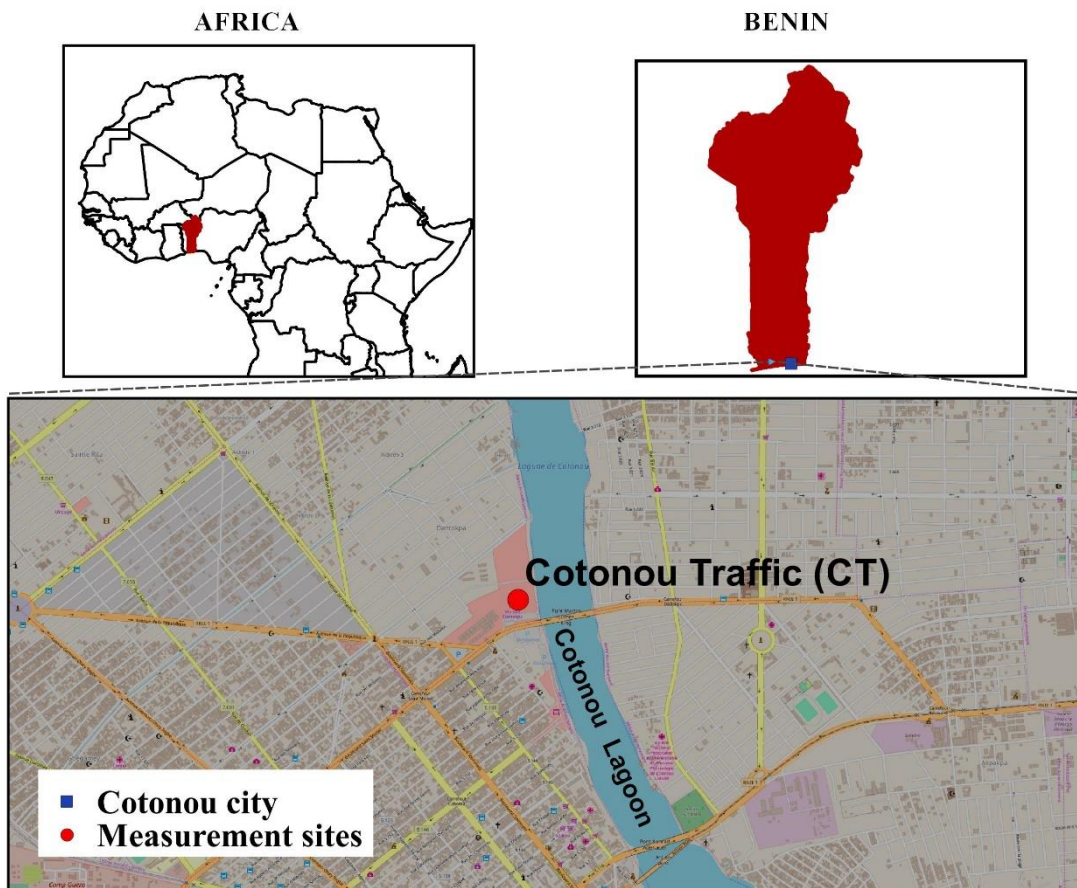
1299

1300

1301   **Figure 2**

1302

1303

1304

1305

1306

1307
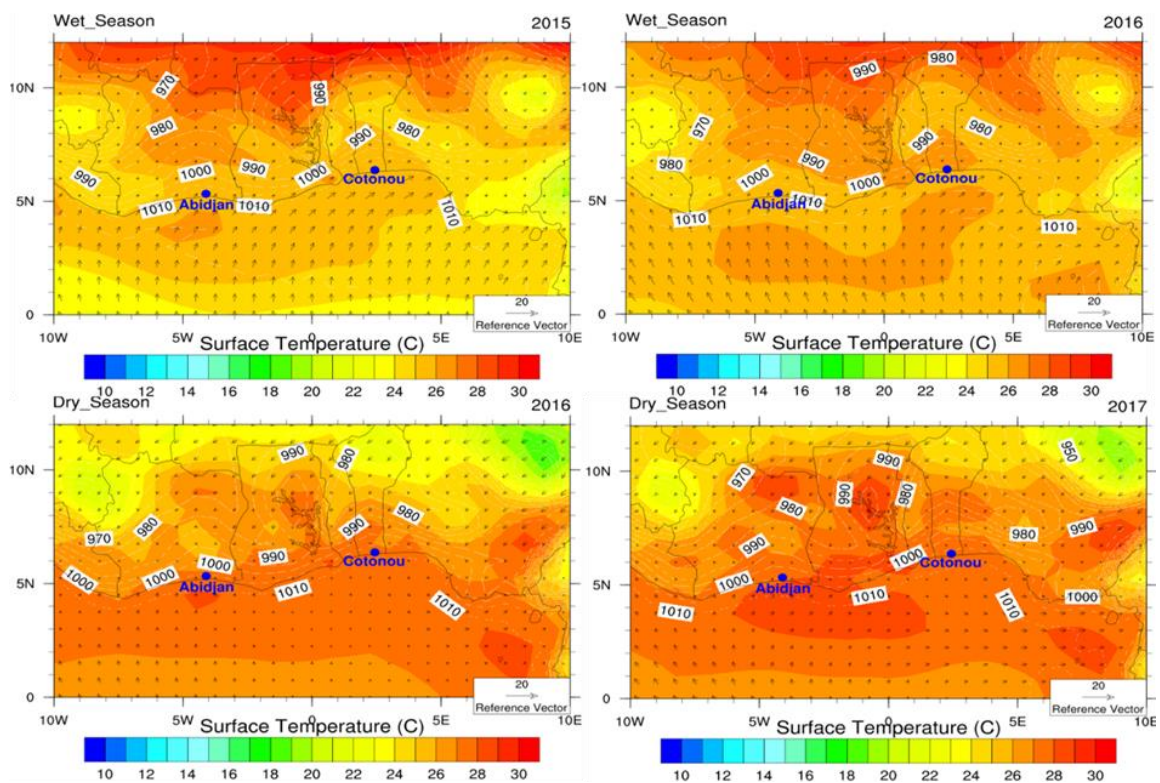
Figure 3

1319

1320

1321 **Figure 4**

1322

1323

1324

1325

1326

1327

1328

1329

1330

1331

1332

1333

1334

1335

1336

1337

Wet season 2015   Wet season 2016

Dry season 2016   Dry season 2017

Figure 5-a

Wet season 2015   Wet season 2016

Dry season 2016   Dry season 2017
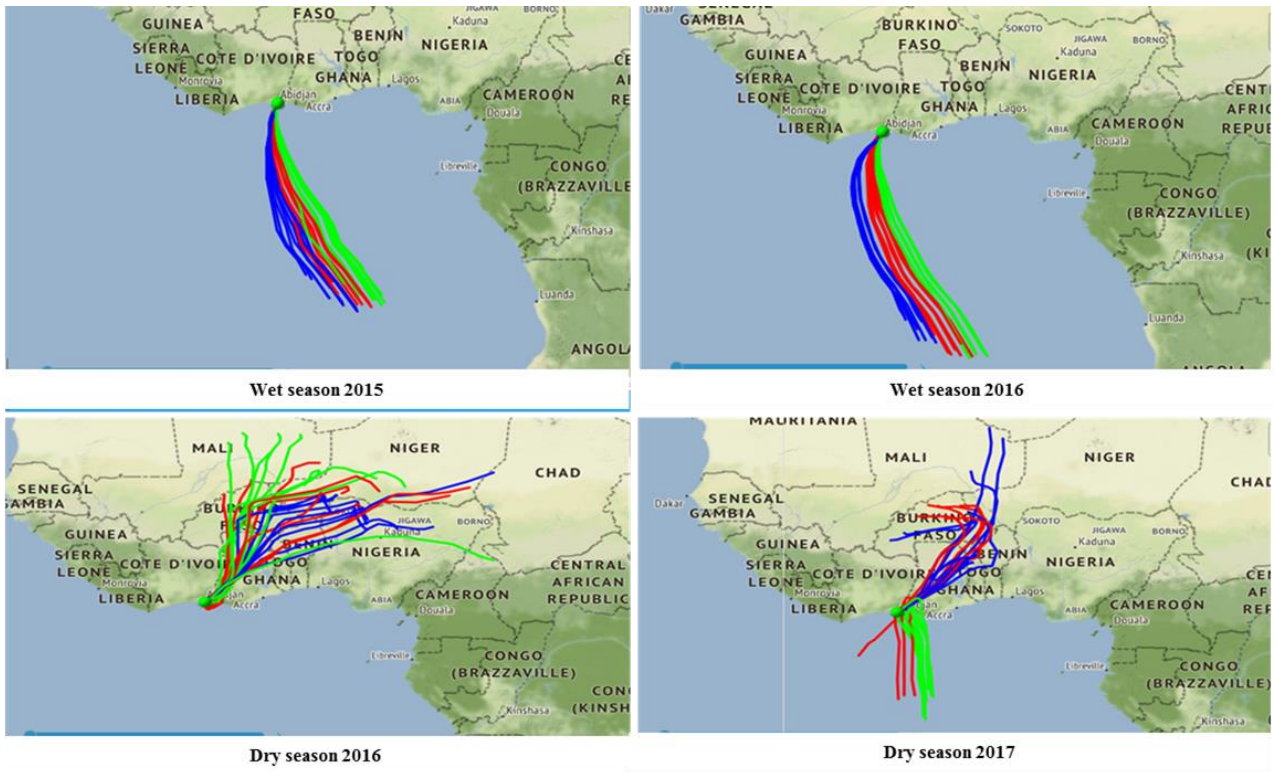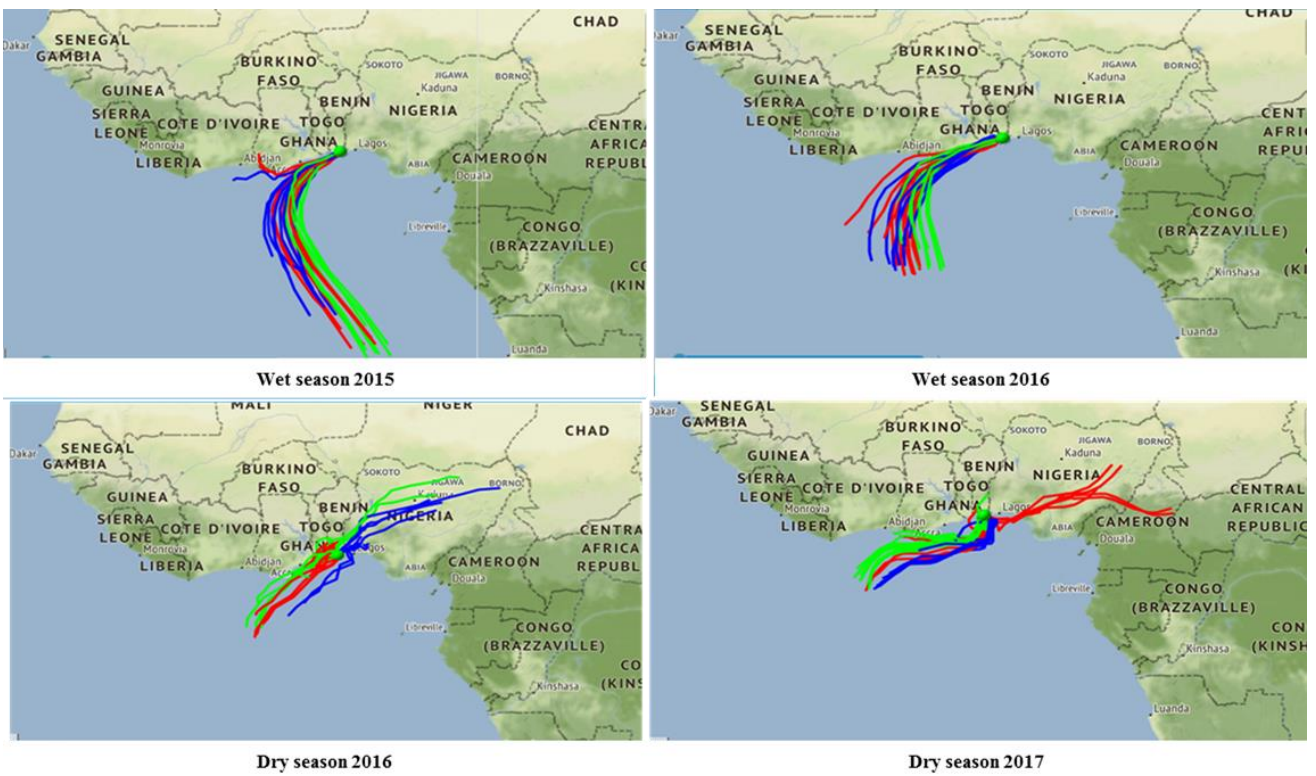
Figure 5-b

1345
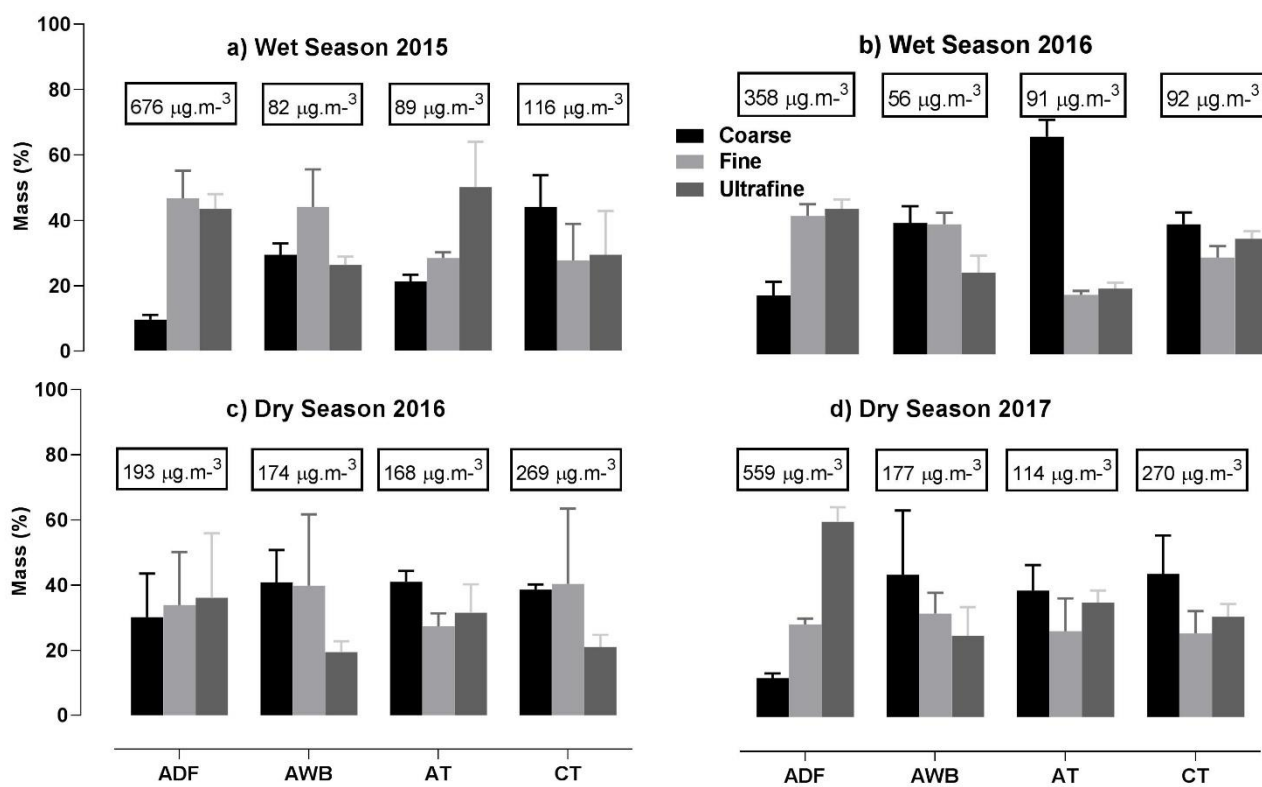
1346

1347 **Figure 6**

1348

1349
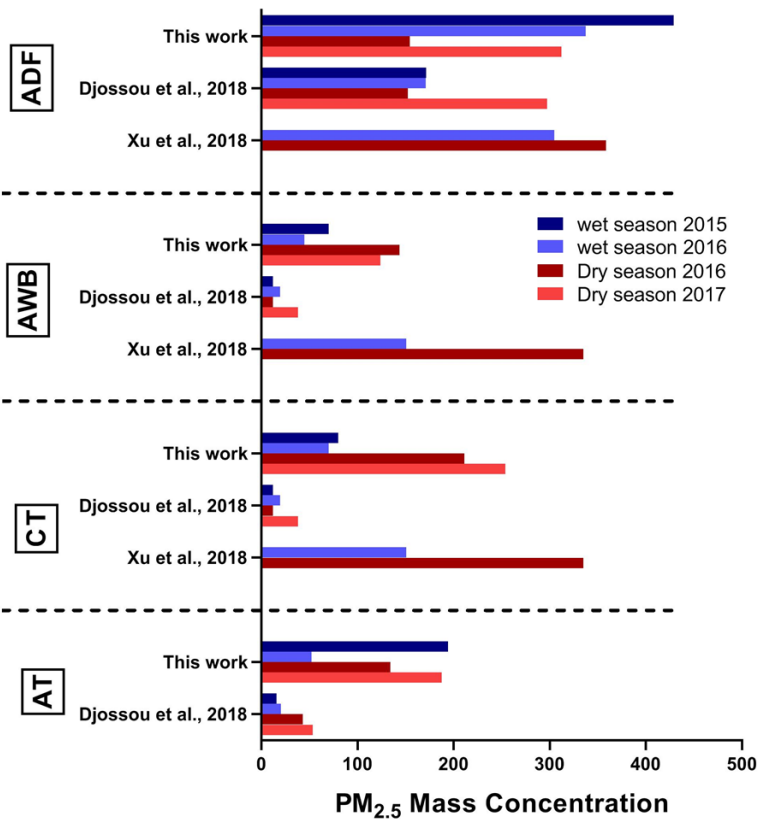
1350

1351 **Figure 7**

1352

1353

1354

1355
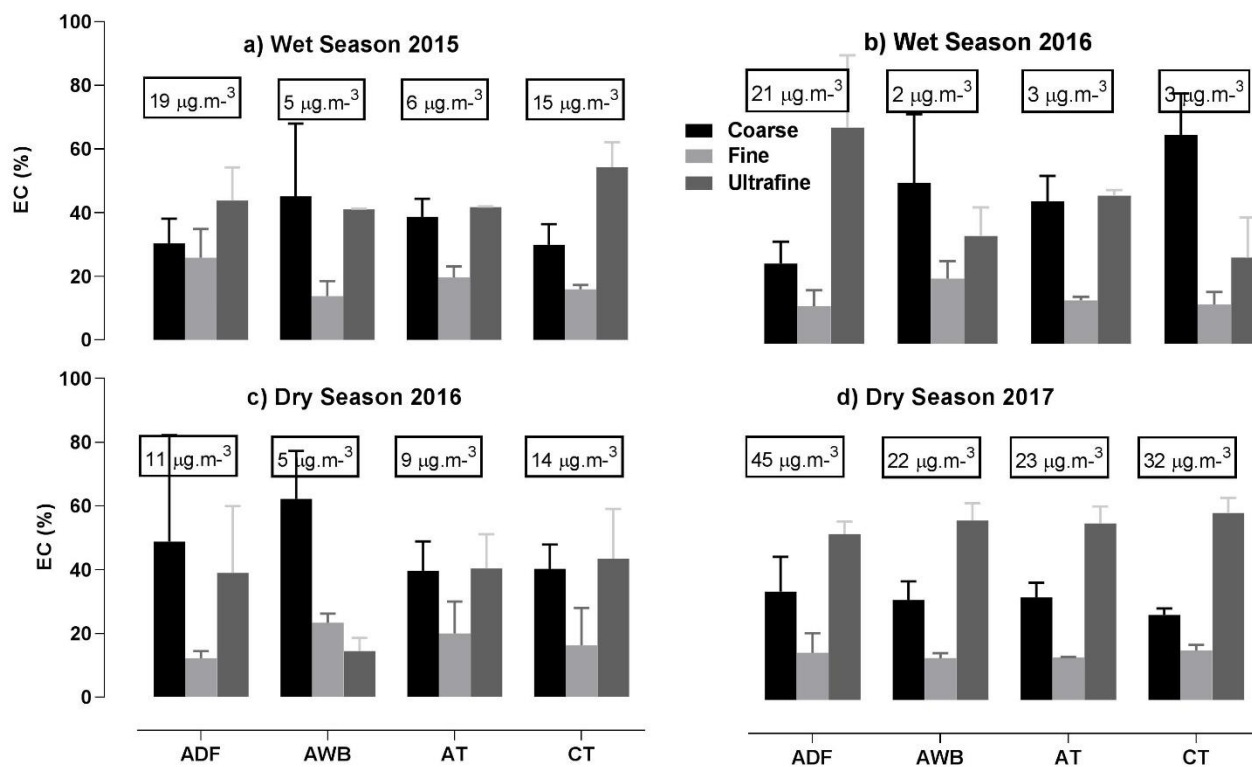
1356

1357   **Figure 8**

1358

1359

1360

1361

1362
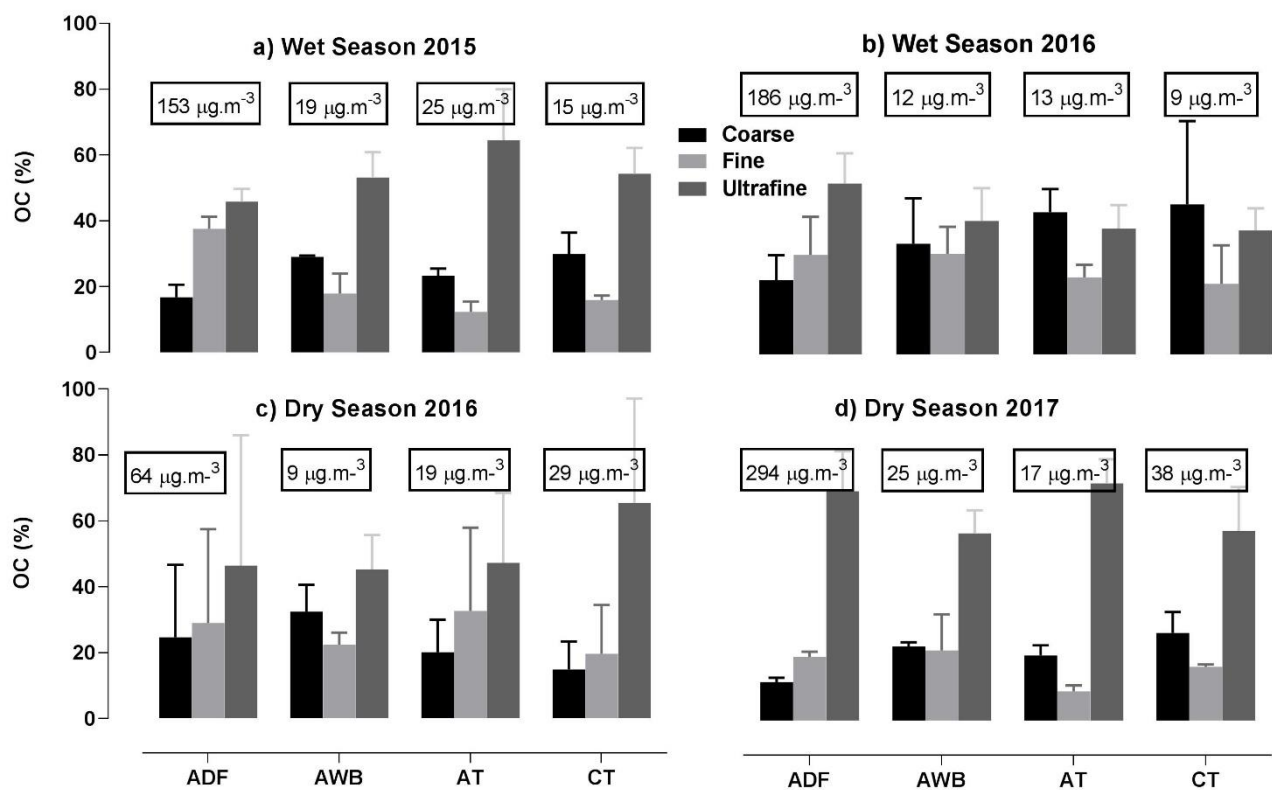
1363

1364   **Figure 9**

1365

1366

1367

1368

1369
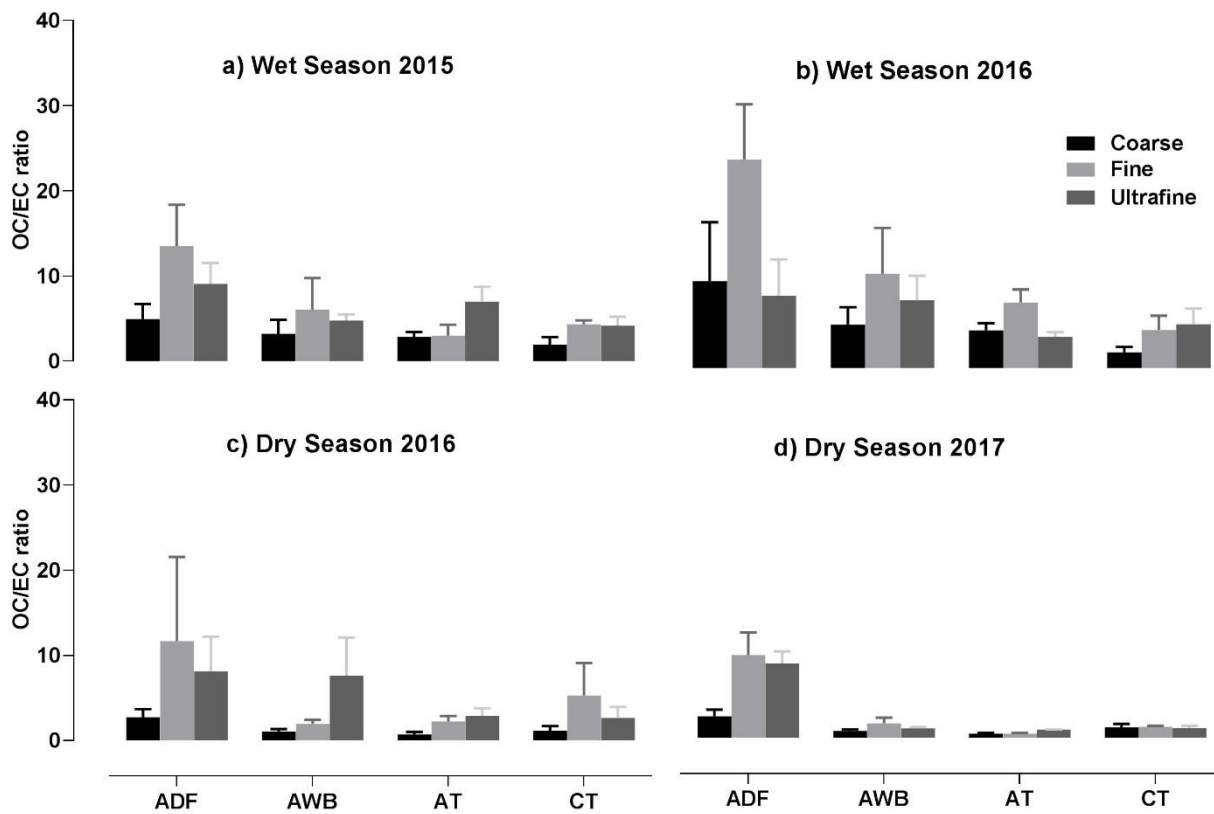
1370

1371   **Figure 10**

1372

1373
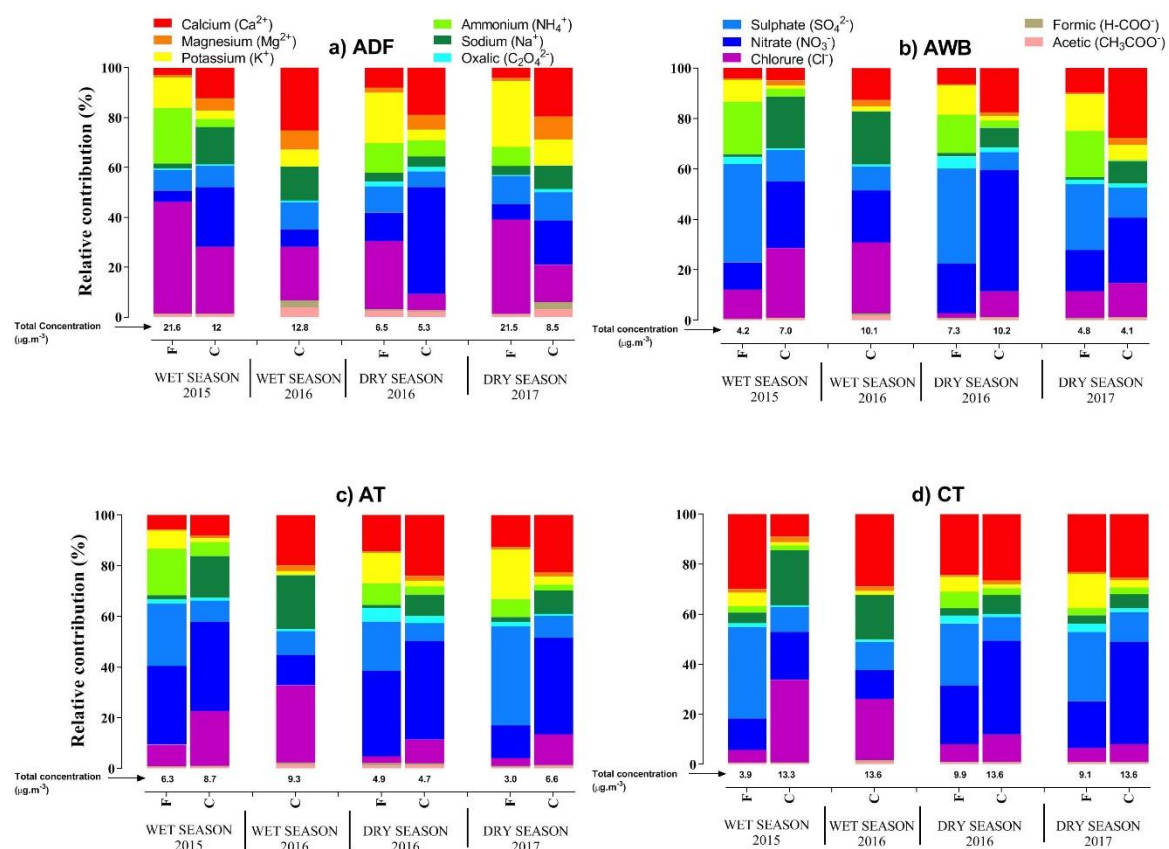
1374

Figure 11

1376

1377
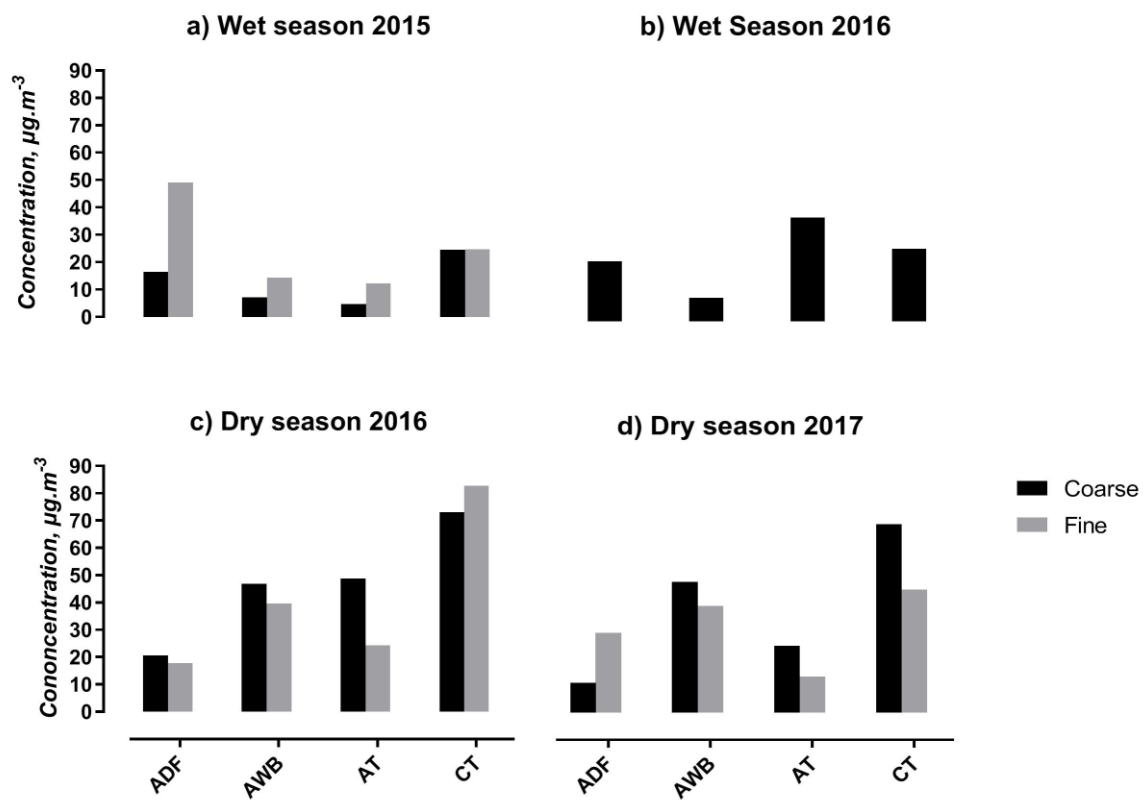
1378

1379 **Figure 12**

1380
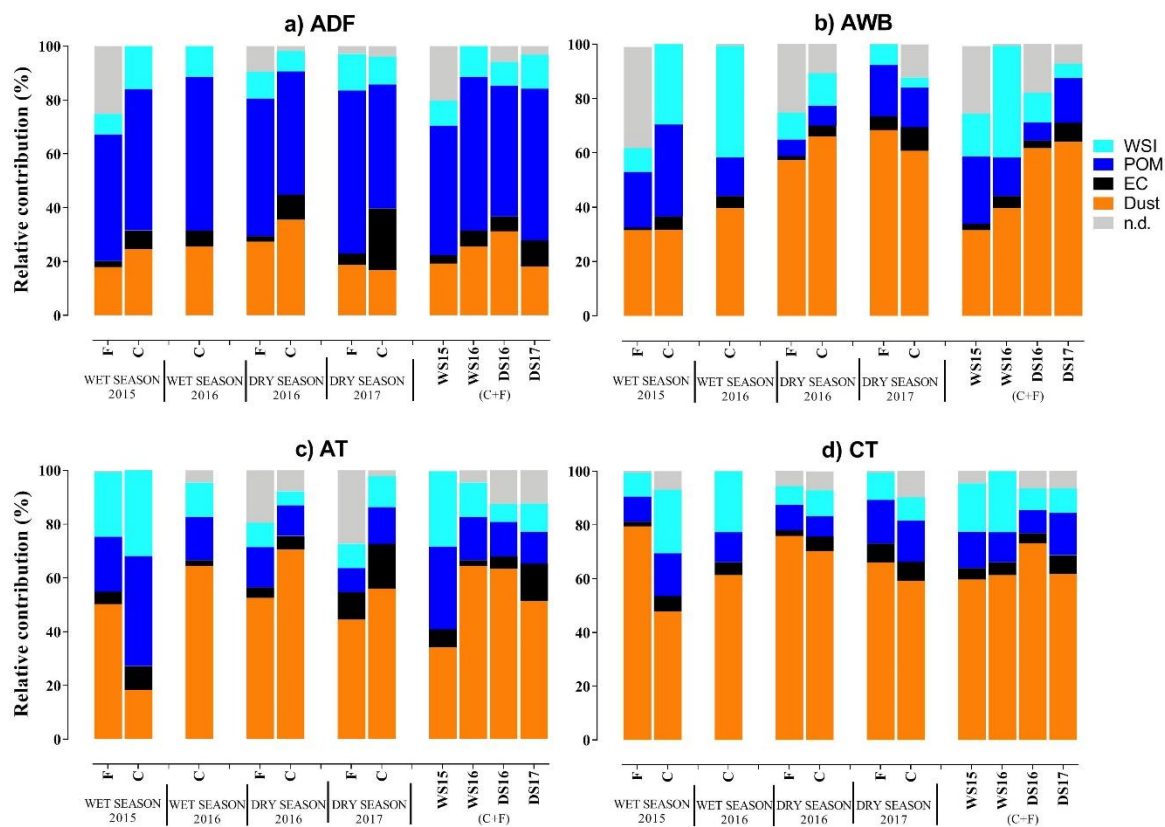
1381

Figure 13

1382

1383

1384

1385

1386
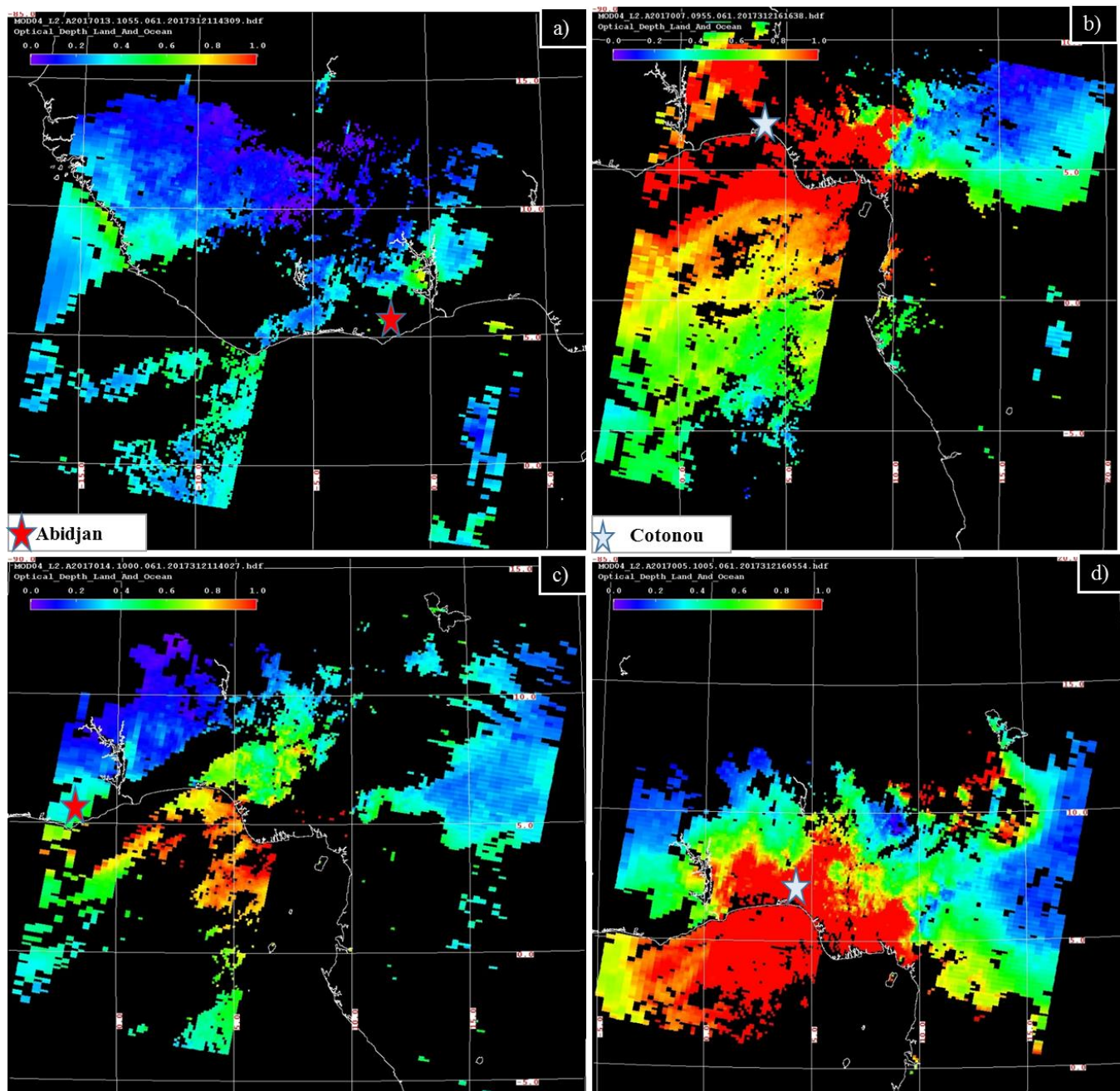
Figure 14

1398   List of table

1399

1400   Table 1: Comparison of dust concentrations obtained from different methodologies

1401   Table 2: WSOC concentrations (μg.m^{-3}) and WSOC/OC ratios (%) for each site, each campaign and
1402   each aerosol size

1403   Table 3: Trace element concentrations for bulk aerosol for each site and for DS2017 and WS2016.

1404   Table 4: Comparison of PM2.5 concentrations with literature data

1405   Table 5: PM2.5-EC and PM2.5-OC comparison with Djossou et al. (2018) and Xu et al. (2019) values.
1406   Units are μgC.m^{-3}

1407   Table 6: EC and OC comparison with literature values

1408   Table 7: Comparison of WSOC concentrations with literature data

1409

1410

1411

1412

1413

1414

1415

1416

1417

1418

1419

1420

1421

1422

1423

1424

1425

1426

1427

1428

1429

1430

1431

1432

1433   Table 1: Comparison of dust concentrations obtained from different methodologies in µg.m^{-3}

Dry 2017		Sciare et al. (2005)	Guinot et al. (2007)	Terzi et al. (2010)
ADF	C	18.5	11.2	86.9
	F	9.3	29.7	22.2
	bulk	27.7	40.9	109.1
AWB	C	12.3	48.5	126.4
	F	5.2	39.7	106.4
	bulk	17.6	88.2	232.8
AT	C	16.4	24.8	98.5
	F	4.3	13.4	34.2
	bulk	20.7	38.2	132.7
CT	C	37.9	70.0	98.4
	F	23.4	45.6	55.8
	bulk	61.3	115.6	154.2

1434

Wet 2016		Sciare et al., 2005	Guinot et al., 2007	Terzi et al.(2010)
ADF	C	35.34	21.5	27.9
AWB	C	13.46	8.6	21.1
AT	C	19.65	37.5	21.4
CT	C	42.98	26.2	52.5
	Bulk	42.98	26.2	52.5

1435

1436

1437

1438

1439

1440

1441

1442

1443 Table 2: WSOC concentrations (µg.m^{-3}) and WSOC/OC ratios (%) for each site, each campaign and

1444 each aerosol size

Site		Abidjan Waste Burning		Abidjan Domestic Fire	
Period	**Size**	**WSOC**	**WSOC/OC**	**WSOC**	**WSOC/OC**
Wet season 2015	Coarse	1.3	24,6	8.2	32.5
	Fine	0.7	19.9	12.8	22.7
	Ultra fine	4.1	43.6	51.3	72.5
	PM2.5	5.5	33.7	69.5	47.2
Dry season 2016	Coarse	0.4	12.3	4.4	18.8
	Fine	0.9	46.9	7.0	20.4
	Ultra fine	1.5	38.4	21.9	61.5
	PM2.5	2.7	32.7	31.0	32.0
Wet season 2016	Coarse	1.3	42.5	16.5	44.3
	Fine	0.8	26.3	17.1	33.0
	Ultra fine	2.0	41.2	79.7	84.5
	PM2.5	3.5	37.1	106.0	52.0
Dry season 2017	Coarse	1.9	32.9	12.1	36.0
	Fine	1.4	38.4	19.9	35.0
	Ultra fine	1.6	11.5	38.6	19.0
	PM2.5	4.0	30.0	65.8	29.0

1445

1446

1447 Table 2 (suite): WSOC concentrations (µg.m^{-3}) and WSOC/OC ratios (%) for each site, each campaign

1448 and each aerosol size

Site		Abidjan Traffic		Cotonou Traffic	
Period	**Size**	**WSOC**	**WSOC/OC**	**WSOC**	**WSOC/OC**
Wet season 2015	Coarse	2.4	39.6	1.1	23.3
	Fine	1.3	46.7	0.5	22.1
	Ultra fine	4.7	29.0	0.4	12.7
	PM2.5	6.9	34.0	2.2	18.0
Dry season 2016	Coarse	1.4	43.0	2.3	64.1
	Fine	1.9	59.0	0.6	10.5
	Ultra fine	4.9	62.0	6.3	42.9
	PM2.5	7.5	49.4	8.0	29.0
Wet season 2016	Coarse	1.1	23.1	1.2	34.7
	Fine	0.5	16.8	0.5	32.2
	Ultra fine	1.4	34.8	0.9	23.0
	PM2.5	2.4	26.0	1.9	28.0
Dry season 2017	Coarse	0.9	24.0	3.5	37.8
	Fine	0.3	24.3	2.4	39.6
	Ultra fine	1.8	14.8	1.9	10.4
	PM2.5	2.6	16.0	6.0	18.2

1449   Table 3: Trace element concentrations for bulk aerosol for each site and for DS2017 and WS2016.

	Bulk ng.m⁻³ (%)							
	DRY 2017				WET 2016			
	ADF	AWB	AT	CT	ADF	AWB	AT	CT
Al	10050.8 (1.8)	25186.1 (13.7)	14015.8 (12.26)	15480.4 (5.7)	1370.5 (0.4)	1990.1 (3.5)	2191.4 (2.4)	4010.5 (4.4)
K	8634.3 (1.5)	6093.7 (3.3)	3677.7 (3.22)	5068.9 (1.9)	1105.0 (0.3)	472.0 (0.8)	275.9 (0.3)	1076.0 (1.2)
Na	6847.8 (1.2)	23430.5 (12.8)	15372.1 (13.44)	11529.3 (4.3)	2070.6 (0.6)	3735.4 (6.6)	2861.5 (3.1)	5310.2 (5.8)
Ca	4321.2 (0.8)	2923.7 (1.6)	4117.6 (3.60)	6233.5 (2.3)	4124.7 (1.1)	447.5 (0.8)	374.7 (0.4)	4954.02 (5.4
Mg	1940.6 (0.3)	384.0 (0.2)	410.3 (0.36)	823.2 (0.3)	1524.7 (0.4)	294.9 (0.5)	283.5 (0.3)	619.2 (0.7)
Fe	1709.9 (0.3)	3807.9 (2.1)	1628.1 (1.42)	3406.8 (1.3)	1314.0 (0.4)	709.3 (1.3)	987.3 (1.1)	1549.4 (1.7)
P	1521.9 (0.3)	696.0 (0.4)	147.8 (0.13)	207.4 (0.1)	605.4 (0.2)	8.6	13.2	81.4 (0.1)
Ti	488.9 (0.1)	2270.3 (1.2)	282.8 (0.25)	457.9 (0.17)	170.8 (0.05)	75.7 (0.13)	96.8 (0.11)	154.7 (0.17)
Zn	189.7 (0.03)	80.9 (0.04)	57.9 (0.05)	149.4 (0.06)	60.3 (0.02)	1.9	41.1 (0.04)	36.2 (0.04)
Zr	172.1 (0.03)	390.3 (0.21)	217.9 (0.19)	145.3 (0.05)	-	22.4 (0.04)	36.7 (0.04)	31.2 (0.03)
Pb	87.1 (0.02)	11.0 (0.01)	4.8	11.5	8.3	2.1	2.3	9.3 (0.01)
Sn	79.7 (0.01)	38.4 (0.02)	21.6 (0.02)	37.4 (0.01)	0.77	0.09	0.0006	9.ç (0.01)
Mn	74.2 (0.01)	35.2 (0.02)	33.7 (0.03)	160.6 (0.06)	48.9 (0.01)	12.01 (0.02)	9.1 (0.01)	41.41 (0.05)
Rb	52.4 (0.01)	8.7	5.9 (0.01)	8.5	4.47	0.71	0.85	1.9
Sb	59.9 (0.01)	201.2 (0.11)	123.6 (0.11)	149.04 (0.06)	24.4 (0.01)	0	0.0006	2.9
Ba	37.3 (0.01)	53.3 (0.03)	47.4 (0.04)	65.8 (0.02)	18.5	8.02 (0.01)	9.9 (0.01)	32.0 (0.03)
Ni	36.5 (0.01)	34.5 (0.02)	27.9 (0.02)	50.2 (0.02)	18.00)	33.1 (0.06)	9.7 (0.01)	14.9 (0.02)
Cr	29.4 (0.01)	53.8 (0.03)	35.8 (0.03)	28.6 (0.01)	41.9 (0.01)	47.7 (0.08)	24.3 (0.03)	29.7 (0.03)
Sr	28.1 (0.01)	15.5 (0.01)	21.2 (0.02)	34.02 (0.01)	17.02	0	0.19	8.1 (0.01)
Cu	24.0	12.3 (0.01)	3.6	9.6	3.99	0.26	0.87	2.8)
Sr	12.6	-	-	-	17.1	-	0.22	8.9 (0.01)
Li	7.3	15.5 (0.01)	7.8 (0.01)	7.39	0.36	0.32	0.23	0.75
Cd	6.1	1.6	1.0	0.83	1.18	0.05	0.02	0.17
V	5.5	12.4 (0.01)	5.1	10.62	2.14	1.84	2.0	3.35
Mo	5.5	8.0	4.9	3.19	4.56	6.84 (0.01)	2.04	3.2
Cs	5.4	0.9	1.2	0.94	0.11	0.12	0.01	0.17
Hf	4.5	10.8 (0.01)	6.8 (0.01)	4.63	0	0.67	1.03	0.97
As	4.2	4.5	3.1	1.22	0	0 (0)	0.05	0.60
Li	4.0	9.8	5.9 (0.01)	5.82	0.27	0.37	0.16	0.93
Co	3.8	1.1	2.1	35.67 (0.01)	0.86	0.49	0.13	0.33
Ce	3.7	6.8	6.0 (0.01)	9.85	1.06	0.50	0.42	2.03
La	1.8	3.5	2.9	4.78	0.54	0.24	0.25	0.92
Nb	1.5	2.6)	1.4	2.48	0.98	0.46	0.5	0.63
Nd	1.5	2.5	2.4	4.15	0.05	0 (0)	-	0.40
Sc	0.69	1.4	1.1)	1.31		0,00		0.02
Be	0.13	0.19	0.2	0.28	0.003	-	-	0.03
Ga	0.61	1.15	0.8	0.98	0.2	0.11	0.12	0.37
Ge	0.42	1.02	0.8	0.68	0.01	0.07	0.02	0.11
Se	0.91	-	-	0.02	0.59	-	0.20	0.18
Rh	0.02	0.02	0.00002	0.002	-	0.002		0.0002
Te	0.06	0.08	0.08	0.05	0.02	0.02	0.02	0,00
Pr	0.40	0.74	0.7	1.13	0.06	0.01	0.004	0.15
Sm	0.27	0.46	0.45	0.76	0.01	0,00	-	0.07
Eu	0.05	0.08	0.08	0.15	0.01	0.003	-	0.0
Gd	0.31	0.57	0.54	0.86	0.05	0.02	0.001	0.15
Tb	0.04	0.07	0.07	0.10	0.005	-	-	0.02
Dy	0.24	0.42	0.40	0.57	0.001	-	-	0.05
Ho	0.05	0.09	0.09	0.12	0.01	0.008	0.01	0.03
Er	0.16	0.31	0.28	0.35	0.02	0.03	0.02	0.09

Tm	0.02	0.05	0.05	0.05	0.002	0.003	0.001	0.01
Yb	0.18	0.38	0.32	0.34	0.01	0.02	0.03	0.09
Lu	0.03	0.06	0.08	0.06	0.003	0.005	0.005	0.02
Ta	0.07	0.14	0.09	0.16	0.06	0.02	0.02	0.03
W	0.80	1.63	0.69	0.54	0.26	0.41	0.4	0.3
Tl	0.22	0.01	0.03	0.06		0.009		
Bi	0.32	0.26	0.02	0.08	0.06	-	-	0.08
Th	0.41	0.88	0.79	1.29	0.15	0.09	0.09	0.24
U	0.22	0.43	0.49	0.51	0.03	0.03	0.02	0.09
Total	36459.9	65817.6	40312.2	44159.2	12562.9	7874.7	7227.2	18001.1
Mass($\mu g/m^3$)	558.8	183.6	114.4	270.0	374.7	56.3	91.6	91.9

1450

1451

1452

1453

1454

1455

1456

1457

1458

1459

1460

1461

1462

1463

1464

1465

1466

1467

1468

1469

1470

1471

1472

1473

1474

1475

1476

1477   Table 4: Comparison of PM2.5 concentrations with literature data

Location	PM2.5 ($\mu g.m^{-3}$)	Reference
Abidjan, Côte d'Ivoire	142	This work
Cotonou, Benin	154	This work
Beijing, China	81.4	Xie et al., 2019
Christchurch, New Zealand	9.2	Tunno et al., 2019
Pune, India	98 ± 28	Pipal et al., 2019
Delhi, India	123	Guttikunda and Calori, 2013
Lahore, Pakistan	91	Colbeck et al., 2011
Ahvaz, Iran	69	Shahsavani et al., 2012
Hong Chong, Hong Kong	54.7 ± 25.6	Cheng et al., 2015
Lecce, Italia	16	Cesari et al., 2016
Libreville, Gabon	35.8	Ngo et al., 2019
Port Gentille, Gabon	60.9	Ngo et al., 2019
Kenitra, Morocco	51.3	Zghaid et al., 2009
Bilecik, Turkey	247	Gaga et al., 2018
Algiers, Algeria	34.8	Bouhila et al., 2015
Shobra, Egypt	216	Lowenthal et al.,2015

1478

1479

1480

1481

1482

1483

1484

1485

1486

1487

1488

1489

1490

1491

1492

1493

1494

1495

1496

1497 Table 5: PM2.5-EC and PM2.5-OC comparison with Djossou et al. (2018) and Xu et al. (2019) values.
1498 Units are $\mu gC.m^{-3}$.

Location	Period	PM2.5 OC	PM2.5 EC	References
Traffic Abidjan. Cote d'Ivoire	July 2015	22.6 ± 3.4	4.3 ± 0.2	This Work
	January 2016	15.2 ± 5.3	7.0 ± 2.6	
	July 2016	9.3 ± 1.3	2.2 ± 0.1	
	January 2017	16.1 ± 1.7	18.9 ± 1.4	
	July 2015	3.3 ± 0.2	2.3 ± 0.2	Djossou et al. 2018
	January 2016	7.7 ± 0.0	3.9 ± 0.0	
	July 2016	7.6 ± 0.2	4.9 ± 0.0	
	January 2017	19.1 ± 6.2	13.9 ± 5.5	
Traffic Cotonou. Benin	July 2015	13.1 ± 1.2	3.5 ± 0.7	This Work
	January 2016	27.8 ± 11.3	10.9 ± 2.6	
	July 2016	6.7 ± 1.9	2.0 ± 0.5	
	January 2017	33.1 ± 4.6	27.3 ± 0.9	
	July 2015	4.2 ± 0.7	1.5 ± 0.1	Djossou et al. 2018
	January 2016	3.0 ± 0.3	1.5 ± 0.2	
	July 2016	6.7 ± 0.2	1.6 ± 0.1	
	January 2017	14.5 ± 0.8	4.4 ± 0.7	
	January 2016	49.5 ± 12.5	13.6 ± 3.6	Xu et al. 2019
	July 2016	37.0 ± 3.5	9.3 ± 0.8	
Domestic fire Abidjan. Cote d'Ivoire	July 2015	147.2 ± 14.5	16.1 ± 1.6	This Work
	January 2016	56.5 ± 51.5	7.4 ± 3.1	
	July 2016	172.3 ± 39.0	17.9 ± 4.8	
	January 2017	283.9 ± 34.9	37.9 ± 4.3	
	July 2015	80.5 ± 1.1	32.2 ± 1.6	Djossou et al. 2018
	January 2016	76.3 ± 13.7	11.4 ± 0.2	
	July 2016	68.4 ± 16.5	17.4 ± 2.1	
	January 2017	66.4 ± 7.5	21.1 ± 6.6	
	January 2016	72.4 ± 24.6	19.5 ± 7.3	Xu et al. 2019
	July 2016	189.3 ± 197.8	11.5 ± 10.8	
Waste Burning Abidjan. Cote d'Ivoire	July 2015	14.8 ± 1.1	4.4 ± 0.1	This Work
	January 2016	7.7 ± 1.3	3.0 ± 0.3	
	July 2016	10.0 ± 2.4	1.5 ± 0.3	
	January 2017	21.9 ± 4.2	19.2 ± 2.4	
	July 2015	3.7 ± 2.2	4.3 ± 0.3	Djossou et al. 2018
	January 2016	13.9 ± 9.0	3.6 ± 1.8	
	July 2016	9.8 ± 4.4	2.8 ± 0.9	
	January 2017	22.4 ± 7.8	8.7 ± 3.0	
	January 2016	85 ± 57.4	15 ± 4.7	Xu et al. 2019
	July 2016	65.2± 65.2	12.3 ± 11.4	

1499

1500

1501

1502   Table 6: EC and OC comparison with literature values

Location	OC (µg.m⁻³)	BC (µg.m⁻³)	Reference
Abidjan (Côte d'Ivoire)	16	8.1	This study
Cotonou (Benin)	20.2	11	This study
Bilecik (Turkey)	49.6-62.8	38.8-58.1	Gaga et al., 2018
Pune (India)	30	5	Pipal et al., 2019
Shanghai (China)	4.9-13.1	1.9-5	Ding et al., 2017
Lahore (Pakistan)	85.7-152	13.8-21	Stone et al., 2010
Agra (India)	25.4-70	3.3-9.5	Satsangi et al., 2012, Pipal et al., 2014
Delhi (India)	34.1-50	5.3-10.6	Bisht et al., 2015a, Pipal et al., 2014
Ahmedabad (India)	18.3	3	Rengarajan et al., 2011
Yokohama (Japan)	4	2	Khan et al., 2010
Beijing (China)	2.9-28.2	1.2-16.3	Guinot et al., 2007

1503

1504

1505

1506

1507

1508

1509

1510

1511

1512

1513

1514

1515

1516

1517

1518

1519

1520

1521

1522

1523

1524   Table 7: Comparison of WSOC concentrations with literature data

Location	WSOC ($\mu g.m^{-3}$)	Reference
Abidjan, Côte d'Ivoire	2-8	This work
Cotonou, Benin	2-8	This work
Beijing, China	9-27	Yu et al., 2018
Beijing, China	4-6	Xiang et al., 2017
Beijing, China	8-12	Tang et al., 2016
Beijing, China	7	Du et al., 2014
Beijing, China	6-8	Feng et al., 2006
Shanghai, China	2-7	Feng et al., 2006, Huang et al., 2012
Guangzhou, Hong Kong	2	Huang et al., 2012
Guangzhou, Hong Kong	5-10	Feng et al., 2006
Gwangju, Korea	2-3.5	Park et al., 2015
Tokyo, Japan	3-23	Sempere and Kawamura, 1994
Cairo, Egypt	3	Favez et al., 2008
Amsterdam, Netherland	1-2	Feng et al., 2007
Barcelone, Spain	1-2	Viana et al., 2007 and 2008
Brindisi, Italy	1.5	Genga et al., 2017
Saint Jean de Maurienne, France	1-5	Sullivan et al., 2004, Jaffrezo et al., 2005a

1525